bioRxiv preprint doi: https://doi.org/10.1101/2021.12.06.471529; this version posted December 7, 2021. The copyright holder for this preprint (which was not certified by peer review) is the author/funder, who has granted bioRxiv a license to display the preprint in perpetuity. It is made available under aCC-BY 4.0 International license.

Decoding the absolute stoichiometric composition and structural plasticity of α-carboxysomes

Yaqi Sun[1], Victoria M. Harman[2], James R. Johnson[3], Taiyu Chen[1,4], Gregory F. Dykes[1], Yongjun Lin[4], Robert J. Beynon[2], Lu-Ning Liu[1,5]*

[1] Institute of Systems, Molecular and Integrative Biology, University of Liverpool, Crown Street, Liverpool L69 7ZB, United Kingdom

[2] Centre for Proteome Research, Institute of Integrative Biology, University of Liverpool, Crown Street, L697ZB, Liverpool, United Kingdom

[3] GeneMill, University of Liverpool, Institute of Integrative Biology, University of Liverpool, Crown Street, L697ZB, Liverpool, United Kingdom

[4] National Key Laboratory of Crop Genetic Improvement and National Center of Plant Gene Research, Huazhong Agricultural University, Wuhan 430070, China

[5] College of Marine Life Sciences, and Frontiers Science Center for Deep Ocean Multispheres and Earth System, Ocean University of China, Qingdao 266003, China

* Correspondence: luning.liu@liverpool.ac.uk (L.-N.L.)

Abstract

Carboxysomes are anabolic bacterial microcompartments that play an essential role in carbon fixation in cyanobacteria and some chemoautotrophs. This self-assembling organelle encapsulates the key CO_2-fixing enzymes, Rubisco, and carbonic anhydrase using a polyhedral protein shell that is constructed by hundreds of shell protein paralogs. The α-carboxysome from the chemoautotroph *Halothiobacillus neapolitanus* serves as a model system in fundamental studies and synthetic engineering of carboxysomes. Here we adopt a QconCAT-based quantitative mass spectrometry to determine the absolute stoichiometric composition of native α-carboxysomes from *H. neapolitanus*. We further performed an in-depth comparison of the protein stoichiometry of native and recombinant α-carboxysomes heterologously generated in *Escherichia coli* to evaluate the structural variability and remodeling of α-carboxysomes. Our results provide insight into the molecular principles that mediate carboxysome assembly, which may aid in rational design and reprogramming of carboxysomes in new contexts for biotechnological applications.

bioRxiv preprint doi: https://doi.org/10.1101/2021.12.06.471529; this version posted December 7, 2021. The copyright holder for this preprint (which was not certified by peer review) is the author/funder, who has granted bioRxiv a license to display the preprint in perpetuity. It is made available under aCC-BY 4.0 International license.

Introduction

Bacterial microcompartments (BMCs) are self-assembling proteinaceous organelles that are widespread among bacterial phyla (Axen et al., 2014; Sutter et al., 2021). The BMC is composed of a virus-like polyhedral protein shell that sequesters a series of enzymes to segregate their metabolic processes from the cytoplasm and provide specific local microenvironments to favor enzymatic activities (Kerfeld et al., 2018; Liu, 2021a; Liu, 2021b; Yeates et al., 2008). Increasing evidence has been achieved to highlight the significant roles of BMCs in enhancing the metabolism of various carbon sources, alleviating metabolic crosstalk, and encapsulating toxic/volatile metabolites (Bobik et al., 2015; Chowdhury et al., 2014; Greening and Lithgow, 2020).

Carboxysomes are anabolic BMCs for autotrophic CO_2 fixation in all identified cyanobacteria and some chemoautotrophs (Borden and Savage, 2021; Kerfeld et al., 2018; Liu, 2021a; Rae et al., 2013; Sun et al., 2020). They encase the CO_2-fixing enzymes, Ribulose-1,5-bisphosphate carboxylase oxygenase (Rubisco) and carbonic anhydrase (CA), using a semi-permeable shell, which allows the passage of negatively charged HCO_3^- and Ribulose 1,5-bisphosphate (RuBP) and probably preclude O_2 influx and leakage of CO_2 from the carboxysome to the cytoplasm (Dou et al., 2008; Faulkner et al., 2020; Mahinthichaichan et al., 2018). In the carboxysome lumen, HCO_3^- is dehydrated to CO_2 by CA, ensuring elevated CO_2 levels around Rubisco to facilitate Rubisco carboxylation and reduce wasteful photorespiration (Long et al., 2021; Price et al., 2008). Collectively, the intriguing self-assembly and selective permeability features of carboxysomes provide the structural basis for enhanced CO_2 assimilation and substantial contributions to global primary production (Hennacy and Jonikas, 2020; Rae et al., 2013; Rae et al., 2017).

According to the forms of encapsulated Rubisco and protein composition, carboxysomes can be categorized into two sub-classes, α- and β-carboxysomes (Kerfeld and Melnicki, 2016; Rae et al., 2013). The α-carboxysome of the chemoautotrophic bacterium *Halothiobacillus neapolitanus* (hereafter as *H. neapolitanus*) has been chosen as a model carboxysome in fundamental studies and synthetic engineering. The genes encoding α-carboxysome-related proteins are clustered mainly in the *cso* operon in the *H. neapolitanus* genome (Figure 1). The shell is constructed by six types of paralogous proteins, including the hexameric proteins (BMC-H) CsoS1A, CsoS1B and CsoS1C that tile the major facet of shells, the pentamers (BMC-P) CsoS4A and CsoS4B that sit at the vertexes, and the trimeric pseudo-hexamer (BMC-T) CsoS1D that possesses a larger central pore than other shell proteins, which was proposed to play a role in mediating the passage of large metabolite molecules,

bioRxiv preprint doi: https://doi.org/10.1101/2021.12.06.471529; this version posted December 7, 2021. The copyright holder for this preprint (which was not certified by peer review) is the author/funder, who has granted bioRxiv a license to display the preprint in perpetuity. It is made available under aCC-BY 4.0 International license.

such as RuBP and 3-phosphoglycerate (3-PGA) (Bonacci et al., 2012; Faulkner et al., 2020; Klein et al., 2009; Roberts et al., 2012). Among the BMC-H proteins, CsoS1A and CsoS1C have a high sequence similarity, differing in only 2 amino acids out of 98 (Heinhorst and Cannon, 2020; Tsai et al., 2007), whereas CsoS1B contains a 12-residue C-terminal extension (Tsai et al., 2007). The cargo enzymes include Rubisco and CA. Rubisco is assembled by the large and small subunits CbbL and CbbS that form an L_8S_8 hexadecamer. CsoSCA acts as the functional CA in the α-carboxysome, existing as a dimer (Sawaya et al., 2006), and was suggested to associate with the shell inner surface (Cai et al., 2015; Dou et al., 2008). The linker protein CsoS2 in the *H. neapolitanus* α-carboxysome has two isoforms, a shorter polypeptide CsoS2A (C-terminus truncated) and a full-length CsoS2B, translated via programmed ribosomal frame shifting (Chaijarasphong et al., 2016). CsoS2A and CsoS2B shared the middle region and the N-terminal domain that binds with Rubisco and induces Rubisco condensation (Oltrogge et al., 2020). The C-terminus of CsoS2B, which is absent in CsoS2A, is presumed to bind with the shell and can serve as an encapsulation peptide to recruit non-native cargos (Cai et al., 2015; Li et al., 2020). In addition, CbbO and CbbQ function as the Rubisco activases, forming a bipartite complex comprising one CbbQ hexamer and one CbbO monomer, to remove inhibitors from the Rubisco catalytic site to restore its carboxylation (Chen et al., 2021; Sutter et al., 2015; Tsai et al., 2015; Tsai et al., 2020).

Given the significance of metabolic improvement and synthetic engineering potential, substantial efforts have been made to uncover the assembly and structural principles of carboxysomes. However, our knowledge about the accurate stoichiometric composition of carboxysomes, which plays an essential role in determining their size, shape, structural integrity, permeability, and catalytic performance (Liu et al., 2021), is still primitive. Label-free quantitative mass spectrometry has been used to determine the relative content of protein compositions within the BMCs (Faulkner et al., 2017; Havemann and Bobik, 2003; Long et al., 2005; Mayer et al., 2016). Furthermore, our recent work has applied mass spectrometry-based absolute quantification and a QconCAT (concatamer of standard peptides for absolute quantification) strategy to examine the precise stoichiometric composition of 1,2-propanediol utilization (PDU) metabolosomes from *Salmonella enterica* serovar Typhimurium LT2 (Yang et al., 2020). In addition, fluorescence labeling and microscopic imaging have been utilized to characterize the protein stoichiometry of β-carboxysomes from the cyanobacterium *Synechococcus elongatus* PCC 7942 (Syn7942) (Sun et al., 2019). However, the precise stoichiometric composition of α-carboxysomes has not been well characterized, despite the crude estimates based on protein

bioRxiv preprint doi: https://doi.org/10.1101/2021.12.06.471529; this version posted December 7, 2021. The copyright holder for this preprint (which was not certified by peer review) is the author/funder, who has granted bioRxiv a license to display the preprint in perpetuity. It is made available under aCC-BY 4.0 International license.

electrophoresis profiles reported in previous studies (Cannon and Shively, 1983; Heinhorst et al., 2006a; Roberts et al., 2012).

Here, we perform absolute quantification of protein components within native α-carboxysomes from *H. neapolitanus* and recombinant α-carboxysomes produced in *Escherichia coli* (*E. coli*), using QconCAT-assisted quantitative mass spectrometry in combination with biochemical analysis, electron microscopy (EM) and enzymatic assays. Our results shed light on the molecular principles underlying the assembly and structural plasticity of α-carboxysomes, and provide essential information required for design and engineering of carboxysomes in synthetic biology.

Results

Quantifying the protein stoichiometry of native α-carboxysomes from *H. neapolitanus*

The QconCAT-assisted mass spectrometry approach permitted a precise quantification of the absolute abundance of proteins (Johnson et al., 2021; Rivers et al., 2007; Simpson and Beynon, 2012). This approach has been recently applied to quantify the stoichiometric composition of protein components within the Pdu metabolosome (Yang et al., 2020). To determine the stoichiometry of α-carboxysome components, native α-carboxysomes were first isolated from *H. neapolitanus* using sucrose gradient ultracentrifugation (Figure S1A). Sodium dodecyl sulfate–polyacrylamide gel electrophoresis (SDS-PAGE) indicated that CsoS2A/B, CbbL/S, and CsoS1A/B/C are the major α-carboxysomes proteins (Figure S1B). NADH-coupled CO_2-fixation activity assays confirmed the functionality of isolated α-carboxysomes, with a measured carbon fixation V_{max} of 2.96 ± 0.09 μmol·mg^{-1}·min^{-1}, and $K_{m(\mathrm{RuBP})}$ at 0.20 ± 0.02 mM (n = 4) (Figure S1C). EM showed that the isolated α-carboxysomes form intact and canonical polyhedral shape, with an average diameter of 124.6 ± 9.6 nm (n = 272) (Figure S1D, S1E), consistent with previous results (Holthuijzen et al., 1986; Shively et al., 1973; Sutter et al., 2015).

To establish the accurate stoichiometry of all proteins within the isolated α-carboxysomes, we used high-resolution liquid chromatography-mass spectrometry (LC-MS) calibrated with protein-specific stable-isotope labeled internal standards generated via the QconCAT strategy (Figure 1, Figure S2) (Johnson et al., 2021; Pratt et al., 2006). The designed single QconCAT peptide is composed of 3 unique peptides for CbbL, CbbS, CsoSCA, CbbO, CbbQ, CsoS1D, CsoS4A and CsoS2AB shared region, 2 peptides for CsoS2B and CsoS1ABC shared region, as well as 1 peptide for the CsoS1B and CsoS1AC shared region (Figure S2A, Table S1). Due to the high sequence similarity, CsoS1A and CsoS1C could not be distinguished in the current QconCAT design. The QconCAT peptide also

bioRxiv preprint doi: https://doi.org/10.1101/2021.12.06.471529; this version posted December 7, 2021. The copyright holder for this preprint (which was not certified by peer review) is the author/funder, who has granted bioRxiv a license to display the preprint in perpetuity. It is made available under aCC-BY 4.0 International license.

132 contains peptides of the form II Rubisco CbbM. Since CbbM was not presumed to be a component of
133 the *H. neapolitanus* α-carboxysome (Baker et al., 1998), we used CbbM as a reference to validate the
134 quality of α-carboxysome isolation. The genes encoding these selected peptide candidates were
135 assembled, following the Qbrick assembly strategy (Johnson et al., 2021), to form the QconCAT DNA
136 sequence (Table S2). The designed QconCAT peptide was then produced by cell-free synthesis
137 (Takemori et al., 2017) and was further isolated, validated by SDS-PAGE (Figure S2B).
138
139 MS1 precursor QconCAT quantification was then carried out using four batches of independently
140 isolated α-carboxysomes (Figure 1A, Figure S3). The purified α-carboxysomes were mixed with the
141 QconCAT standard, co-digested, and analyzed by label-free MS quantification. All carboxysomal
142 proteins were detected in the isolated carboxysomes, whereas CbbM was not detectable in the isolated
143 samples. The carboxysomal proteins account for 99.5 ± 0.2% of the total proteins in the samples,
144 confirming the high purity of isolated carboxysomes (Figure S4A). Accuracy and reliability of protein
145 quantification were verified by a good agreement of the peptides for each carboxysome protein in the
146 four biological replicates (Figure S4C).
147
148 We quantified the abundance of protein components within one *H. neapolitanus* carboxysome structure,
149 based on the shell surface area of a typical icosahedron (Whitehead et al., 2014) and the average
150 carboxysome size (124.6 ± 9.6 nm, n = 272) measured in EM (Figure 1C, Table 1, Table S3, see details
151 in Methods). The results revealed that the most abundant proteins in the *H. neapolitanus* α-
152 carboxysome are CsoS1AC hexamers (863 copies), followed by Rubisco (447 copies, estimated by the
153 CbbL content), CsoS2A (248 copies), CsoS2B (192 copies), CsoS1B hexamers (112 copies), and 58
154 copies of CsoSCA dimers. The *H. neapolitanus* α-carboxysome has a molecular weight (MW) of ~346
155 MDa and the Rubisco enzymes account for ~66% of the total MW. The hexameric shell proteins
156 CsoS1A/C and CsoS1B make up ~17.1% of the total MW. Additionally, 11 copies of CsoS4A/B
157 pentamers (CsoS4A: 8.8; CsoS4B: 2.2) are integrated within the α-carboxysome, slightly less than 12
158 that is typically assumed to cap the vertices of an icosahedron. CsoS1D pseudo-hexamers have a low
159 abundance in the shell, with 2.9 copies per carboxysome. Moreover, the linker proteins, CsoS2A and
160 CsoS2B, account for 13.5% of the total MW.
161
162 Approximately 15 copies of CbbQO complexes, each composed of one CbbQ hexamer and one CbbO
163 monomer, were identified in the carboxysome, indicating that the CbbQO complex is a structural
164 component of native α-carboxysomes in *H. neapolitanus*. Consistently, CbbQ has been indicated to be

bioRxiv preprint doi: https://doi.org/10.1101/2021.12.06.471529; this version posted December 7, 2021. The copyright holder for this preprint (which was not certified by peer review) is the author/funder, who has granted bioRxiv a license to display the preprint in perpetuity. It is made available under aCC-BY 4.0 International license.

tightly associated with the *H. neapolitanus* carboxysome shell (Sutter et al., 2015) and CbbQO can be incorporated into recombinant α-carboxysomes (Chen et al., 2021). Likewise, our mass spectrometry results showed the presence of McdAB-like proteins in purified native α-carboxysomes (Figure S4A, Supplemental File 1), implicating the association of McdAB-like proteins with α-carboxysomes, which was proposed to ensure proper distribution of α-carboxysomes in *H. neapolitanus* and carboxysome inheritance during cell division (MacCready et al., 2021). Some chemoautotrophs, including *H. neapolitanus*, contain the *cbbM* gene encoding Form II Rubisco and its activases CbbQ1 and CbbO1 (Tsai et al., 2015). These proteins were not detected in the purified carboxysomes (Supplemental File 1), suggesting that they are not the organizational components of or associated with the α-carboxysomes in *H. neapolitanus*.

Stoichiometric composition of recombinant α-carboxysomes

Previous studies have demonstrated that heterologous engineering of the *H. neapolitanus* α-carboxysomes could result in functional α-carboxysome structures (Baumgart et al., 2017; Bonacci et al., 2012; Chen et al., 2021; Flamholz et al., 2020). To verify the compositional similarity between native and recombinant α-carboxysomes, we reconstituted *H. neapolitanus* α-carboxysomes by expressing the *cso* operon with *csoS1D* using an arabinose-inducible pBAD33 vector in *E. coli* (Figure S1G). SDS-PAGE revealed an overall similar content of protein components within the isolated native and recombinant α-carboxysomes, except for a reduction in the CsoSCA content in recombinant carboxysomes (Figure S1B, S3). Carbon-fixation kinetics as a function of RuBP concentrations confirmed the function of recombinant α-carboxysomes, with a V_{max} of 2.07 ± 0.12 μmol·mg^{-1}·min^{-1} (n = 4) and a $K_{m(\mathrm{RuBP})}$ of 0.08 ± 0.02 mM (n = 4), although both were lower than those of native α-carboxysomes (Figure S1C). EM indicated that recombinant α-carboxysomes possess a polyhedral shape and an average diameter of 131.8 ± 18.0 nm (n = 152), slightly larger than native α-carboxysomes (Figure S1D, S1E). Analysis of EM images showed that both native and recombinant α-carboxysomes possess single-layer shells (5.3 ± 0.6 nm and 5.5 ± 0.8 nm, respectively, n = 100, Figure S1F), consistent with previous observations (Faulkner et al., 2017).

Isolated recombinant α-carboxysomes were then subject to MS1 precursor QconCAT quantification and normalization to retrieve the stoichiometric content of a single carboxysome (Figure 1, Table 2, Table S3). Within the recombinant α-carboxysome, the most abundant proteins are CsoS1AC hexamers (1001 copies), followed by Rubisco (426 copies), CsoS2A (305 copies), CsoS2B (249 copies), and CsoS1B hexamers (79 copies). The recombinant α-carboxysome has a molecular mass of ~336 MDa,

bioRxiv preprint doi: https://doi.org/10.1101/2021.12.06.471529; this version posted December 7, 2021. The copyright holder for this preprint (which was not certified by peer review) is the author/funder, who has granted bioRxiv a license to display the preprint in perpetuity. It is made available under aCC-BY 4.0 International license.

and has significantly reduced Rubisco copy numbers compared with the native α-carboxysome ($p < 0.05$, Figure 2). The content of CsoSCA in the recombinant α-carboxysome is reduced by 29-fold compared to that in the native α-carboxysome, resulting in only ~2 CsoSCA dimers per recombinant α-carboxysome, consistent with SDS-PAGE analysis (Figure S1B). The hexameric shell proteins, CsoS1AC and CsoS1B, account for 19.4% of the total MW in recombinant α-carboxysomes (Table 2). The CsoS1B content is reduced by ~30% (79 copies) compared to that in native α-carboxysomes (112 copies, $p < 0.05$, Figure 2). There are on average 7.1 copies of pentameric proteins (CsoS4A: 6.3; CsoS4B: 0.8) in recombinant α-carboxysomes, less than the hypothetical 12 pentamers for a typical icosahedral structure. It suggests that some vertices are not capped by CsoS4 pentamers. Similar features have also been observed in β-carboxysomes and synthetic BMC shells (Hagen et al., 2018; Sun et al., 2019; Sutter et al., 2019), presumably providing a mechanism for regulating shell architecture and permeability. CsoS1D has ~0.8 copies per recombinant α-carboxysome, less than that in the native α-carboxysome ($p < 0.001$, Table 2). CsoS2A and CsoS2B have 305 and 249 copies, respectively, per recombinant α-carboxysome, collectively accounting for 17.6% of the total MW. CsoS2B has an increased content in the recombinant α-carboxysome than in the native form (Figure 2).

Discussion

In this study, we performed absolute quantification using QconCAT-based mass spectrometry to determine the stoichiometric composition of the *H. neapolitanus* α-carboxysomes, which represent a step toward gaining a comprehensive understanding of the structure and function of the model carboxysome.

Given that BMC components have a notable variation in protein abundance (Yang et al., 2020) and some minor proteins were not identifiable as well as the protein paralogs with similar molecular were not distinguishable in SDS-PAGE gels (Figure 1, Figure S2), it is difficult to obtain the accurate protein stoichiometry of carboxysomes based on protein electrophoresis profiles. Comparison of QconCAT and label-free quantification results illustrated marked deviations in the abundance of some carboxysomal proteins (Figure S4B). The results demonstrated that label-free quantification could potentially underestimate the content of CsoS1B, CsoSCA, CsoS4A, and CsoS4B by 48/32%, 64/95%, 144/142%, and 119/105% (native/recombinant carboxysomes), respectively, highlighting the necessity of QconCAT-based quantification in studying the protein stoichiometric composition of BMCs.

Stoichiometric variability and structural plasticity of α-carboxysomes

bioRxiv preprint doi: https://doi.org/10.1101/2021.12.06.471529; this version posted December 7, 2021. The copyright holder for this preprint (which was not certified by peer review) is the author/funder, who has granted bioRxiv a license to display the preprint in perpetuity. It is made available under aCC-BY 4.0 International license.

Characterization of the absolute stoichiometric compositions for native and recombinant carboxysomes provides insight into the organizational principles and plasticity of the *H. neapolitanus* α-carboxysome (Figure 3). It becomes apparent that the BMC shells are amendable to integrate different copies or types of shell proteins, and the absence of specific components or the changes in the ratios of protein paralogs may not necessarily impede the overall shell assembly (Garcia-Alles et al., 2019; Long et al., 2018; Sommer et al., 2019; Yang et al., 2020). The total copy number of shell pentamers (CsoS4A and CsoS4B) is 11.0 for native α-carboxysomes and 7.1 for recombinant α-carboxysomes, both less than 12 pentamers that are postulated to occupy all the vertices of a regular icosahedron (Bobik et al., 2015; Kerfeld et al., 2018). These results elucidated that it is not a prerequisite to cap all the vertices with pentamers in a functional carboxysome. In support of this, polyhedral carboxysomes and BMC shells deficient in pentamers could still be formed (Cai et al., 2009; Hagen et al., 2018; Lassila et al., 2014; Long et al., 2018). Our previous study has also demonstrated that variable copies of CcmL pentamers are integrated in Syn7942 β-carboxysomes under different growth conditions (Sun et al., 2019). The lack of pentamers at some vertices might result in observable structural heterogeneity and reduced integrity of the entire α-carboxysomes (Figure S1D).

Rubisco in carboxysomes was proposed to adopt a Kepler packing, filling maximally 74% of the internal carboxysome volume (Long et al., 2011; Whitehead et al., 2014). Quantification based upon the CbbL content indicates that the native *H. neapolitanus* α-carboxysome can accommodate approximately 447 Rubisco (the CbbL:CbbS ratio is 8:7.3), in agreement with the theoretical estimation based on the Kepler packing (411 Rubisco, Table S3). In contrast, recombinant α-carboxysomes encapsulate 426 Rubisco (the CbbL:CbbS ratio is 8:5.7), lower than the estimated copy number of 491 based on measured recombinant carboxysome size (Table S3). The increased shell:interior ratio (from 0.8:1 to 1:1, Table. 3) and carboxysome size specified a lower packing density of Rubisco within recombinant carboxysomes (Figure 3). Moreover, the perturbed formation of Rubisco (L_8S_8) as indicated by the changes in the CbbL:CbbS ratio has also been determined in recombinant carboxysomes (Table 3). Our results also showed that the Rubisco/CA (CbbL:CsoSCA) ratio varies drastically between native and recombinant α-carboxysomes (Table 3). It has been postulated that too little or too much carboxysomal CA activity, which could cause limited CO_2 supply or substantial leakage of CO_2, may interfere with CO_2 fixation of carboxysomes (Rae et al., 2013). Other changes that occurred in recombinant carboxysomes involve the increased content of CsoS1 shell proteins, the reduced CsoS1D abundance, as well as the absence of CbbQO (the *cbbQ* and *cbbO* genes were not included in the expression construct) (Figure 3). All these structural alternations may

bioRxiv preprint doi: https://doi.org/10.1101/2021.12.06.471529; this version posted December 7, 2021. The copyright holder for this preprint (which was not certified by peer review) is the author/funder, who has granted bioRxiv a license to display the preprint in perpetuity. It is made available under aCC-BY 4.0 International license.

collectively result in the higher size variation of recombinant α-carboxysomes and the discrepancy in the carbon-fixation performance between native and recombinant α-carboxysomes (Figure S1C-1E).

CsoS2 in α-carboxysomes serve as the scaffolding protein that interlinks Rubisco and shells (Cai et al., 2015; Chaijarasphong et al., 2016; Rae et al., 2013). The CbbL:CsoS2 ratios in native and recombinant α-carboxysomes remain within a narrow range between 8:1 and 8:1.3 (Table 3), implicating the correlation between Rubisco and CsoS2, which is fundamental for Rubisco condensation and internal packing. Likewise, the CsoS2A:CsoS2B ratio remains relatively unaltered in native (ratio of 1.3:1) and recombinant (ratio of 1.2:1) α-carboxysomes.

Organizational features of diverse carboxysomes

Peptide composition of the α-carboxysomes from the α-cyanobacterium *Prochlorococcus marinus* MED4 has been estimated based on standard protein gel profiles (Roberts et al., 2012). The *H. neapolitanus* α-carboxysomes (~125 nm in diameter) are larger in diameter than the *Prochlorococcus* α-carboxysomes (~90 nm in diameter). Consistently, the *H. neapolitanus* α-carboxysome has a 1.8-fold increased content of CsoS1 hexameric shell proteins (975 versus 539 copies) and encapsulates double copy numbers of CsoSCA proteins (58 versus 29) and nearly 3-fold more Rubisco enzymes (447 versus 152 copies). The experimentally determined Rubisco content fits well the theoretical estimate (411 copies for the *H. neapolitanus* carboxysome and 143 copies for the *Prochlorococcus* carboxysome), which were based on the carboxysome size and Kepler packing (Long et al., 2011; Whitehead et al., 2014). In contrast, Pdu microcompartments, with the diameter ranging from 90 to 130 nm, have a drastically higher shell:interior ratio (4.6:1) (Yang et al., 2020) than the *H. neapolitanus* α-carboxysome (0.8:1, Table 3), implying that Kepler packing of cargo enzymes is unlikely applicable to metabolosomes. The CsoSCA:CsoS1 ratio retain relatively constant in both native α-carboxysomes, presumably implicating their specific association within the carboxysomes. In contrast, CA in the Syn7942 β-carboxysomes, which encoded by the *ccaA* gene that is distant from the *ccm* operon, was demonstrated to have a varying abundance per carboxysome under different environmental conditions (Sun et al., 2019). It remains to be investigated if the CsoSCA content in α-carboxysomes is subject to environmental modulation.

A noteworthy feature of the *Prochlorococcus* α-carboxysome is that it contains only the full length of CsoS2 without the short isoform as the *H. neapolitanus* counterpart does, which might lead to formation of carboxysomes with reduced Rubisco loading capacity and overall size. However, the

bioRxiv preprint doi: https://doi.org/10.1101/2021.12.06.471529; this version posted December 7, 2021. The copyright holder for this preprint (which was not certified by peer review) is the author/funder, who has granted bioRxiv a license to display the preprint in perpetuity. It is made available under aCC-BY 4.0 International license.

Rubisco:CsoS2 ratios in the α-carboxysomes from *H. neapolitanus* and *Prochlorococcus* remain relatively comparable (1:1 and 1:1.1, respectively), indicative of a general Rubisco encapsulation mechanism of α-carboxysomes. In the Syn7942 β-carboxysome, the ratio between Rubisco and the scaffolding protein CcmM varied in a range of 1:0.8 to 1:1.3, depending upon environmental conditions (Sun et al., 2019). Unlike the similar CsoS2A:CsoS2B ratios in native and recombinant α-carboxysomes, the CcmM35:CcmM58 ratios in the Syn7942 β-carboxysomes have a wide range of 1:1 to 11:1, and have been proved to be vital for carboxysome assembly (Long et al., 2011; Long et al., 2010).

Carboxysomes are highly modular structures with the capacity of incorporating foreign cargos, representing an ideal system in synthetic biology (Li et al., 2020). Advanced knowledge about the precise protein stoichiometry of functional carboxysome structures is essential for fine-tuning and reprogramming carboxysomes in native and heterogeneous organisms for metabolic enhancement and diverse biotechnological applications in new contexts (Liu et al., 2021). The QconCAT-based protein quantification technique could be broadly used in the studies of diverse BMC paralogs and protein organelles from their native origins and heterologous hosts.

Methods

Bacterial strains, growth conditions and carboxysome production

H. neapolitanus (*Halothiobacillus neapolitanus* Parker, Kelly and Wood ATCC 23641 C2) used in this work was acquired from ATCC (The American Type Culture Collection) as freeze-dried powder (Cannon et al., 2001; Hutchinson et al., 1965). Stock cells were maintained in liquid ATCC medium 290 (Hutchinson et al., 1967) or on ATCC 290 1.5% agar plates. Scale-up culture was grown similar to the protocol described previously (Dou et al., 2008), in the Vishniac and Santer medium (Vishniac and Santer, 1957) in a 5-liter fermenter (BioFlo 115, New Brunswick Scientific, USA) at 30°C. The pH of growth medium was maintained at 7.6 by constant supplement of 3 M KOH. Air supply was set at 500 $L \cdot min^{-1}$ for initial growth and reduced to 200 $L \cdot min^{-1}$ 24-48 hours prior to harvesting. Agitation was kept at 250-300 RPM. For expression of recombinant carboxysomes, the entire *cso* operon, as designed on *pHnCBS1D* reported previously (Bonacci et al., 2012), was fused on a pBAD33 arabinose inducible expression vector (Aigner and Wilson, 2017) using Gibson Assembly strategy (Gibson et al., 2009) with Gibson Assembly® Master Mix from NEB. Primer sets used for assembly were listed in Table S5. For recombinant carboxysome expression in *E. coli*, seeding cultures containing chloramphenicol at a

bioRxiv preprint doi: https://doi.org/10.1101/2021.12.06.471529; this version posted December 7, 2021. The copyright holder for this preprint (which was not certified by peer review) is the author/funder, who has granted bioRxiv a license to display the preprint in perpetuity. It is made available under aCC-BY 4.0 International license.

final concentration of 50 μg mL^{-1} were inoculated at 37°C in LB broth until reaching OD600 at 0.6, and then scaled up for induction with 1mM Arabinose at 20°C overnight.

Carboxysome purification from *H. neapolitanus* and *E. coli*

The α-carboxysome purification from *H. neapolitanus* was modified from the protocol described previously (Heinhorst et al., 2006b). Sulfur-free Cells fractions were obtained by subsequential centrifugation at 12,000 g for 10 min, 300 g for 15 min and 12,000 g for 10 min in TEMB buffer (10 mM Tris-HCl, pH 8.0, 10 mM $MgCl_2$, 20 mM $NaHCO_3$, 1 mM EDTA). Cells in 15ml of TEMB were then incubated with egg lysosome for 1 hour at 30°C, and disrupted via glass beads beating (150-212 μm glass bead, acid washed, Sigma-Aldrich). The lysates were further treated with 33% (v/v) B-PERII (ThermoFisher Scientific, UK) and 0.5% (v/v) IGEPAL CA630 (Sigma-Aldrich) and placed on a rotary mixer for 2 hours. The unbroken cells and large membrane debris were removed by centrifugation at 9,000g for 10min. Crude CB enrichment was pelleted at 48,000 g for 30 min. The pellet was resuspended, briefly centrifuged at 9,000 g and then loaded to a step sucrose gradient (10% 20% 30% 35% 50% 60%) and ultra-centrifuged at 105,000 g for 35 min. The milky layer of enriched carboxysome was harvested at 35%- 50% sucrose layers. Sucrose was removed by an additional round of ultracentrifuge after diluting with TEMB. The pure carboxysome pellet was resuspended in a small volume of TEMB. Unless indicated otherwise, all procedures were performed at 4°C. The carboxysome purification from *E. coli* was performed as described previously (Bonacci et al., 2012; So et al., 2004) with minor modifications. The step gradient of sucrose was kept the same as the one for native carboxysome isolation. Additionally, IGEPAL CA-630 detergent was used at 0.5% (v/v) after cell break to reduce membrane contaminants in final enrichments.

SDS-PAGE analysis

SDS-PAGE were performed following standard procedures. 10 μg purified carboxysomal proteins or 100 μg whole cell fractions were loaded per-well on 15% polyacrylamide gels and stained with Coomassie Brilliant Blue G-250 (ThermoFisher Scientific, UK).

Design, cell-free expression and purification of QconCAT standard

Absolute quantification for the carboxysomal proteins was designed by concatenated signature QconCAT peptides (Pratt et al., 2006) in a similar way to that described previously (Yang et al., 2020). In brief, up to three qualified peptide candidates, when available according to design principles (Pratt et al., 2006) were nominated to quantify each protein (Table S1). Candidate peptides were BLAST

bioRxiv preprint doi: https://doi.org/10.1101/2021.12.06.471529; this version posted December 7, 2021. The copyright holder for this preprint (which was not certified by peer review) is the author/funder, who has granted bioRxiv a license to display the preprint in perpetuity. It is made available under aCC-BY 4.0 International license.

searched against protein database for both *H. neap* and *E. coli* to ensure their uniqueness. Due to the high level of sequence similarity of CsoS1A/B/C, CsoS2A/B and CsoS4A/B, peptides represent shared sequences as well as unique sequences were included (Figure S2). The DNA fragment encoding the above peptides, together with GluFib and cMyc (these peptides are used to quantify the standard) and 6x His-tag on N-terminal and C-terminal respectively were generated following ALACAT/Qbrick assembly strategy as reported previously (Johnson et al., 2021). The final DNA sequence (Table S2) was assembled into a pEU-E01 vector for cell-free expression using wheat germ lysate (CellFree Sciences Co., Ltd, Japan). Synthesis was completed with [$^{13}C_6$, $^{15}N_4$] arginine and [$^{13}C_6$, $^{15}N_2$] lysine (CK Isotopes Ltd, UK) using WEPR8240H full Expression kit following default protocols (2BScientific Ltd, UK). The QconCAT peptides were purified with Ni Sepharose suspension (GE Healthcare Ltd, UK) in centrifuge filters (Corning Costar Spin-X 0.45 um pore size cellulose acetate membrane, Merck, UK) following standard methods. The QconCAT was precipitated and resuspended in 30 µL 25 mM ammonium bicarbonate, with 0.1% (w/v) RapiGestTM SF surfactant (Waters, UK) and protease inhibitors (Roche cOmpleteTM, Mini, EDTA-free Protease Inhibitor Cocktail, Merck, UK).

Proteomic analysis

The protein concentration of each sample was determined using a NanoDrop Spectrophotometer (ThermoFisher Scientific, UK). Protein (0.5 µg) was digested with 0.01 µg Trypsin Gold, Mass Spectrometry Grade (Promega, US) at 37°C overnight after pretreatment with 0.05% (w/v) RapiGestTM SF surfactant at 80°C for 10 mins, 4 mM dithiothreitol (Melford Laboratories Ltd., UK) at 60°C for 10 mins and 14 mM iodoacetamide at room temperature for 30 mins. Digestions were acidified with trifluoroacetic acid (Greyhound Chromatography and Allied Chemicals, UK) and then centrifuged at 13,000 g to remove insoluble, non-peptidic material. Four biological replicates for both native and recombinant carboxysomes were analyzed using an UltiMateTM 3000 RSLCnano system coupled to a Q Exactive™ HF Hybrid Quadrupole-Orbitrap™ Mass Spectrometer (ThermoFisher Scientific, UK) in data-dependent acquisition mode according to the protocol published (Johnson et al., 2021). The LC was operated under the control of Dionex Chromatography MS Link 2.14. The raw MS data files were loaded into Thermo Proteome Discoverer v.1.4 (ThermoFisher Scientific, UK) and searched against carboxysome QconCAT database using Mascot v.2.7 (Matrix Science London, UK) with trypsin as the specified enzyme. Each precursor ion was cleanly isolated using the high-resolution and high-scanning speed of the MS1 approach. A precursor mass tolerance of 10 ppm and a fragment ion mass tolerance of 0.01 Da were applied. Additionally, preparations of the four native and synthetic

bioRxiv preprint doi: https://doi.org/10.1101/2021.12.06.471529; this version posted December 7, 2021. The copyright holder for this preprint (which was not certified by peer review) is the author/funder, who has granted bioRxiv a license to display the preprint in perpetuity. It is made available under aCC-BY 4.0 International license.

carboxysomes were analyzed by label-free quantification. Data analysis, including run alignment and peak picking, was carried out in Progenesis QI for Proteomics v4. The quantification data were also visualized and analyzed using Simplifi (simplify.protifi.com), which are available through permanent hyperlinks included in the text.

For single carboxysome quantitative normalization, relative quantifications from QconCAT were normalized both 12 pentamer coverage, and a single layer shell protein coverage of hexameric and pentameric proteins (Table S4). 12-pentamer normalization is done via assuming 60 copies of monomeric CsoS4A and CsoS4B in sum per carboxysome. For shell coverage normalization, the shell surface area is first calculated using TEM measured diameter with the following formula:

$$A_f = 5\sqrt{3}a^3;\ R_c = \frac{\sqrt{10+2\sqrt{5}}}{4}a$$

whereas A_f is total surface area, a is edge length, and R_c is the circumcized radius (refer to as the diameter). The hexameric counts were then calculated using the total surface area and diameters of CsoS1A hexamers in a layer as reported previously (Tsai et al., 2007).

Electron Microscopy and data analysis

Electron microscopy was carried out as described previously (Faulkner et al., 2017). The purified carboxysomes (~ 4 mg mL^{-1}) were stained with 3% uranyl acetate on carbon grids and then inspected with FEI 120 kV Tecnai G2 Spirit BioTWIN TEM equipped with a Gatan Rio 16 camera. The diameters of carboxysomes were measured with ImageJ as described previously (Faulkner et al., 2017) and were statistically analyzed using Origin (OriginLab, Massachusetts, USA).

Rubisco activity assays

Carbon fixation assay was carried out to determine carbon fixation capacities of purified native and recombinant carboxysomes as described previously using a 3-phosphoglycerate–dependent NADH oxidation coupled enzyme system (Bonacci et al., 2012). For both native and synthetic samples, four biological replicates that were isolated from different culture batches were assayed at 30°C, initiated with final concentrations of 0.0625 mM, 0.125 mM, 0.25 mM, 0.5 mM, 1 mM, and 2 mM of RuBP. The concentration of HCO_3^- was set to 24 mM for all assays in this work.

bioRxiv preprint doi: https://doi.org/10.1101/2021.12.06.471529; this version posted December 7, 2021. The copyright holder for this preprint (which was not certified by peer review) is the author/funder, who has granted bioRxiv a license to display the preprint in perpetuity. It is made available under aCC-BY 4.0 International license.

Acknowledgments

We thank Prof. Ian Prior and Mrs. Alison Beckett for the support of electron microscopy. This work was supported by the National Key R&D Program of China (2021YFA0909600 to L.-N.L.), the National Natural Science Foundation of China (32070109 to L.-N.L.), the Royal Society (URF\R\180030, RGF\EA\181061, RGF\EA\180233 to L.-N.L.), the Biotechnology and Biological Sciences Research Council Grant (BB/V009729/1, BB/M024202/1, BB/R003890/1 to L.-N.L. and BB/S020241/1 to R.J.B.), the Leverhulme Trust (RPG-2021-286 to L.-N.L.), and the International Postdoctoral Exchange Fellowship Program from China Postdoctoral Science Foundation (20180079 to T.C.).

Author contributions

Y.Q., R.J.B. and L.-N.L. designed research; Y.Q., V.M.H., J.R.J., T.C., and G.F.D. performed research; Y.Q., V.M.H., Y.L., R.J.B. and L.-N.L. analyzed data; Y.Q. and L.-N.L. wrote the manuscript with contributions from other authors.

Data availability

The mass spectrometry data are deposited to the public-accessible platform SimpliFi. The data for QconCAT quantification are available at: https://simplifi.protifi.com/#/p/dd32b950-2e5c-11eb-808d-871337eb317b. The data for label-free quantification search against *H. neapolitanus* protein database are available at: https://simplifi.protifi.com/#/p/e527f900-3e50-11eb-808d-871337eb317b. All other data are available from the corresponding author upon request.

Competing Interests

The authors declare no conflict of interest.

bioRxiv preprint doi: https://doi.org/10.1101/2021.12.06.471529; this version posted December 7, 2021. The copyright holder for this preprint (which was not certified by peer review) is the author/funder, who has granted bioRxiv a license to display the preprint in perpetuity. It is made available under aCC-BY 4.0 International license.

References

Aigner, H., and Wilson, R.H. (2017). Plant RuBisCo assembly in E. coli with five chloroplast chaperones including BSD2. 358:1272-1278.

Axen, S.D., Erbilgin, O., and Kerfeld, C.A. (2014). A taxonomy of bacterial microcompartment loci constructed by a novel scoring method. PLoS Comput Biol 10:e1003898.

Baker, S.H., Jin, S., Aldrich, H.C., Howard, G.T., and Shively, J.M. (1998). Insertion mutation of the form I cbbL gene encoding ribulose bisphosphate carboxylase/oxygenase (RuBisCO) in Thiobacillus neapolitanus results in expression of form II RuBisCO, loss of carboxysomes, and an increased CO2 requirement for growth. J Bacteriol 180:4133-4139.

Baumgart, M., Huber, I., Abdollahzadeh, I., Gensch, T., and Frunzke, J. (2017). Heterologous expression of the *Halothiobacillus neapolitanus* carboxysomal gene cluster in *Corynebacterium glutamicum*. J. Biotechnol. 258:126-135.

Bobik, T.A., Lehman, B.P., and Yeates, T.O. (2015). Bacterial microcompartments: widespread prokaryotic organelles for isolation and optimization of metabolic pathways. Mol Microbiol 98:193-207.

Bonacci, W., Teng, P.K., Afonso, B., Niederholtmeyer, H., Grob, P., Silver, P.A., and Savage, D.F. (2012). Modularity of a carbon-fixing protein organelle. Proc Natl Acad Sci U S A 109:478-483.

Borden, J.S., and Savage, D.F. (2021). New discoveries expand possibilities for carboxysome engineering. Curr Opin Microbiol 61:58-66.

Cai, F., Dou, Z., Bernstein, S.L., Leverenz, R., Williams, E.B., Heinhorst, S., Shively, J., Cannon, G.C., and Kerfeld, C.A. (2015). Advances in Understanding Carboxysome Assembly in Prochlorococcus and Synechococcus Implicate CsoS2 as a Critical Component. Life (Basel) 5:1141-1171.

Cai, F., Menon, B.B., Cannon, G.C., Curry, K.J., Shively, J.M., and Heinhorst, S. (2009). The pentameric vertex proteins are necessary for the icosahedral carboxysome shell to function as a CO_2 leakage barrier. PLoS One 4:e7521.

Cannon, G.C., and Shively, J.M. (1983). Characterization of a homogenous preparation of carboxysomes from *Thiobacillus neapolitanus*. Archives of Microbiology 134:52-59.

Chaijarasphong, T., Nichols, R.J., Kortright, K.E., Nixon, C.F., Teng, P.K., Oltrogge, L.M., and Savage, D.F. (2016). Programmed Ribosomal Frameshifting Mediates Expression of the alpha-Carboxysome. J Mol Biol 428:153-164.

Chen, T., Fang, Y., Jiang, Q., Dykes, G.F., Lin, Y., Price, G.D., Long, B.M., and Liu, L.N. (2021). Incorporation of Functional Rubisco Activases into Engineered Carboxysomes to Enhance Carbon Fixation. ACS Synth Biol:https://doi.org/10.1021/acssynbio.1021c00311.

Chowdhury, C., Sinha, S., Chun, S., Yeates, T.O., and Bobik, T.A. (2014). Diverse bacterial microcompartment organelles. Microbiol Mol Biol Rev 78:438-468.

Dou, Z., Heinhorst, S., Williams, E.B., Murin, C.D., Shively, J.M., and Cannon, G.C. (2008). CO2 fixation kinetics of Halothiobacillus neapolitanus mutant carboxysomes lacking carbonic anhydrase suggest the shell acts as a diffusional barrier for CO2. J Biol Chem 283:10377-10384.

Faulkner, M., Rodriguez-Ramos, J., Dykes, G.F., Owen, S.V., Casella, S., Simpson, D.M., Beynon, R.J., and Liu, L.-N. (2017). Direct characterization of the native structure and mechanics of cyanobacterial carboxysomes. Nanoscale 9:10662–10673.

Faulkner, M., Szabó, I., Weetman, S.L., Sicard, F., Huber, R.G., Bond, P.J., Rosta, E., and Liu, L.-N. (2020). Molecular simulations unravel the molecular principles that mediate selective permeability of carboxysome shell protein. Scientific Reports 10:17501.

Flamholz, A.I., Dugan, E., Blikstad, C., Gleizer, S., Ben-Nissan, R., Amram, S., Antonovsky, N., Ravishankar, S., Noor, E., Bar-Even, A., et al. (2020). Functional reconstitution of a bacterial CO2 concentrating mechanism in Escherichia coli. Elife 9.

Garcia-Alles, L.F., Root, K., Maveyraud, L., Aubry, N., Lesniewska, E., Mourey, L., Zenobi, R., and Truan, G. (2019). Occurrence and stability of hetero-hexamer associations formed by beta-carboxysome CcmK shell components. PLoS One 14:e0223877.

bioRxiv preprint doi: https://doi.org/10.1101/2021.12.06.471529; this version posted December 7, 2021. The copyright holder for this preprint (which was not certified by peer review) is the author/funder, who has granted bioRxiv a license to display the preprint in perpetuity. It is made available under aCC-BY 4.0 International license.

Gibson, D.G., Young, L., Chuang, R.Y., Venter, J.C., Hutchison, C.A., 3rd, and Smith, H.O. (2009). Enzymatic assembly of DNA molecules up to several hundred kilobases. Nat Methods 6:343-345.

Greening, C., and Lithgow, T. (2020). Formation and function of bacterial organelles. Nature Reviews Microbiology 18:677-689.

Hagen, A., Sutter, M., Sloan, N., and Kerfeld, C.A. (2018). Programmed loading and rapid purification of engineered bacterial microcompartment shells. Nat Commun 9:2881.

Havemann, G.D., and Bobik, T.A. (2003). Protein content of polyhedral organelles involved in coenzyme B12-dependent degradation of 1,2-propanediol in Salmonella enterica serovar Typhimurium LT2. J Bacteriol 185:5086-5095.

Heinhorst, S., and Cannon, G.C. (2020). Bacterial Microcompartments. In: Bacterial Organelles and Organelle-like Inclusions--Jendrossek, D., ed. Cham: Springer International Publishing. 125-147.

Heinhorst, S., Cannon, G.C., and Shively, J.M. (2006a). Carboxysomes and Carboxysome-like Inclusions. In: Complex Intracellular Structures in Prokaryotes--Shively, J.M., ed. Berlin, Heidelberg: Springer Berlin Heidelberg. 141-165.

Heinhorst, S., Williams, E.B., Cai, F., Murin, C.D., Shively, J.M., and Cannon, G.C. (2006b). Characterization of the carboxysomal carbonic anhydrase CsoSCA from Halothiobacillus neapolitanus. J Bacteriol 188:8087-8094.

Hennacy, J.H., and Jonikas, M.C. (2020). Prospects for Engineering Biophysical CO_2 Concentrating Mechanisms into Land Plants to Enhance Yields. Annu Rev Plant Biol 71:461-485.

Holthuijzen, Y.A., van Breemen, J.F.L., Konings, W.N., and van Bruggen, E.F.J. (1986). Electron microscopic studies of carboxysomes of *Thiobacillus neapolitanus*. Archives of Microbiology 144:258-262.

Johnson, J., Harman, V.M., Franco, C., Emmott, E., Rockliffe, N., Sun, Y., Liu, L.-N., Takemori, A., Takemori, N., and Beynon, R.J. (2021). Construction of à la carte QconCAT protein standards for multiplexed quantification of user-specified target proteins. BMC Biology 19:195.

Kerfeld, C.A., Aussignargues, C., Zarzycki, J., Cai, F., and Sutter, M. (2018). Bacterial microcompartments. Nat Rev Microbiol 16:277-290.

Kerfeld, C.A., and Melnicki, M.R. (2016). Assembly, function and evolution of cyanobacterial carboxysomes. Curr Opin Plant Biol 31:66-75.

Klein, M.G., Zwart, P., Bagby, S.C., Cai, F., Chisholm, S.W., Heinhorst, S., Cannon, G.C., and Kerfeld, C.A. (2009). Identification and structural analysis of a novel carboxysome shell protein with implications for metabolite transport. J Mol Biol 392:319-333.

Lassila, J.K., Bernstein, S.L., Kinney, J.N., Axen, S.D., and Kerfeld, C.A. (2014). Assembly of robust bacterial microcompartment shells using building blocks from an organelle of unknown function. J Mol Biol 426:2217-2228.

Li, T., Jiang, Q., Huang, J., Aitchison, C.M., Huang, F., Yang, M., Dykes, G.F., He, H.-L., Wang, Q., Sprick, R.S., et al. (2020). Reprogramming bacterial protein organelles as a nanoreactor for hydrogen production. Nature Communications 11:5448.

Liu, L.N. (2021a). Advances in the bacterial organelles for CO_2 fixation. Trends in Microbiology https://doi.org/10.1016/j.tim.2021.10.004.

Liu, L.N. (2021b). Bacterial metabolosomes: new insights into their structure and bioengineering. Microbial Biotechnology 14:88-93.

Liu, L.N., Yang, M., Sun, Y., and Yang, J. (2021). Protein stoichiometry, structural plasticity and regulation of bacterial microcompartments. Curr Opin Microbiol 63:133-141.

Long, B.M., Forster, B., Pulsford, S.B., Price, G.D., and Badger, M.R. (2021). Rubisco proton production can drive the elevation of CO_2 within condensates and carboxysomes. Proc Natl Acad Sci U S A 118:e2014406118.

Long, B.M., Hee, W.Y., Sharwood, R.E., Rae, B.D., Kaines, S., Lim, Y.L., Nguyen, N.D., Massey, B., Bala, S., von Caemmerer, S., et al. (2018). Carboxysome encapsulation of the CO2-fixing enzyme Rubisco in tobacco chloroplasts. Nat Commun 9:3570.

bioRxiv preprint doi: https://doi.org/10.1101/2021.12.06.471529; this version posted December 7, 2021. The copyright holder for this preprint (which was not certified by peer review) is the author/funder, who has granted bioRxiv a license to display the preprint in perpetuity. It is made available under aCC-BY 4.0 International license.

Long, B.M., Price, G.D., and Badger, M.R. (2005). Proteomic assessment of an established technique for carboxysome enrichment from Synechococcus PCC7942. Canadian Journal of Botany 83:746-757.

Long, B.M., Rae, B.D., Badger, M.R., and Price, G.D. (2011). Over-expression of the beta-carboxysomal CcmM protein in Synechococcus PCC7942 reveals a tight co-regulation of carboxysomal carbonic anhydrase (CcaA) and M58 content. Photosynth Res 109:33-45.

Long, B.M., Tucker, L., Badger, M.R., and Price, G.D. (2010). Functional cyanobacterial beta-carboxysomes have an absolute requirement for both long and short forms of the CcmM protein. Plant Physiol 153:285-293.

MacCready, J.S., Tran, L., Basalla, J.L., Hakim, P., and Vecchiarelli, A.G. (2021). The McdAB system positions alpha-carboxysomes in proteobacteria. Mol Microbiol 116:277-297.

Mahinthichaichan, P., Morris, D.M., Wang, Y., Jensen, G.J., and Tajkhorshid, E. (2018). Selective Permeability of Carboxysome Shell Pores to Anionic Molecules. The journal of physical chemistry. B 122:9110-9118.

Mayer, M.J., Juodeikis, R., Brown, I.R., Frank, S., Palmer, D.J., Deery, E., Beal, D.M., Xue, W.F., and Warren, M.J. (2016). Effect of bio-engineering on size, shape, composition and rigidity of bacterial microcompartments. Sci Rep 6:36899.

Oltrogge, L.M., Chaijarasphong, T., Chen, A.W., Bolin, E.R., Marqusee, S., and Savage, D.F. (2020). Multivalent interactions between CsoS2 and Rubisco mediate α-carboxysome formation. Nature structural & molecular biology 27:281-287.

Pratt, J.M., Simpson, D.M., Doherty, M.K., Rivers, J., Gaskell, S.J., and Beynon, R.J. (2006). Multiplexed absolute quantification for proteomics using concatenated signature peptides encoded by QconCAT genes. Nat Protoc 1:1029-1043.

Price, G.D., Badger, M.R., Woodger, F.J., and Long, B.M. (2008). Advances in understanding the cyanobacterial CO2-concentrating-mechanism (CCM): functional components, Ci transporters, diversity, genetic regulation and prospects for engineering into plants. J Exp Bot 59:1441-1461.

Rae, B.D., Long, B.M., Badger, M.R., and Price, G.D. (2013). Functions, compositions, and evolution of the two types of carboxysomes: polyhedral microcompartments that facilitate CO2 fixation in cyanobacteria and some proteobacteria. Microbiol Mol Biol Rev 77:357-379.

Rae, B.D., Long, B.M., Forster, B., Nguyen, N.D., Velanis, C.N., Atkinson, N., Hee, W.Y., Mukherjee, B., Price, G.D., and McCormick, A.J. (2017). Progress and challenges of engineering a biophysical CO_2-concentrating mechanism into higher plants. J Exp Bot 68:3717-3737.

Rivers, J., Simpson, D.M., Robertson, D.H., Gaskell, S.J., and Beynon, R.J. (2007). Absolute multiplexed quantitative analysis of protein expression during muscle development using QconCAT. Molecular & cellular proteomics : MCP 6:1416-1427.

Roberts, E.W., Cai, F., Kerfeld, C.A., Cannon, G.C., and Heinhorst, S. (2012). Isolation and characterization of the Prochlorococcus carboxysome reveal the presence of the novel shell protein CsoS1D. J Bacteriol 194:787-795.

Sawaya, M.R., Cannon, G.C., Heinhorst, S., Tanaka, S., Williams, E.B., Yeates, T.O., and Kerfeld, C.A. (2006). The structure of beta-carbonic anhydrase from the carboxysomal shell reveals a distinct subclass with one active site for the price of two. J Biol Chem 281:7546-7555.

Shively, J.M., Ball, F.L., and Kline, B.W. (1973). Electron microscopy of the carboxysomes (polyhedral bodies) of *Thiobacillus neapolitanus*. J Bacteriol 116:1405-1411.

Simpson, D.M., and Beynon, R.J. (2012). QconCATs: design and expression of concatenated protein standards for multiplexed protein quantification. Analytical and bioanalytical chemistry 404:977-989.

So, A.K., Espie, G.S., Williams, E.B., Shively, J.M., Heinhorst, S., and Cannon, G.C. (2004). A novel evolutionary lineage of carbonic anhydrase (epsilon class) is a component of the carboxysome shell. J Bacteriol 186:623-630.

Sommer, M., Sutter, M., Gupta, S., Kirst, H., Turmo, A., Lechno-Yossef, S., Burton, R.L., Saechao, C., Sloan, N.B., Cheng, X., et al. (2019). Heterohexamers formed by CcmK3 and CcmK4 increase the complexity of beta carboxysome Shells. Plant Physiol 179:156-167.

bioRxiv preprint doi: https://doi.org/10.1101/2021.12.06.471529; this version posted December 7, 2021. The copyright holder for this preprint (which was not certified by peer review) is the author/funder, who has granted bioRxiv a license to display the preprint in perpetuity. It is made available under aCC-BY 4.0 International license.

Sun, Y., Huang, F., and Liu, L.-N. (2020). Self-Assembly, Organisation, Regulation, and Engineering of Carboxysomes: CO2-Fixing Prokaryotic Organelles. In: Microbial Photosynthesis--Wang, Q., ed. Singapore: Springer Singapore. 319-343.

Sun, Y., Wollman, A.J.M., Huang, F., Leake, M.C., and Liu, L.N. (2019). Single-Organelle Quantification Reveals Stoichiometric and Structural Variability of Carboxysomes Dependent on the Environment. Plant Cell 31:1648-1664.

Sutter, M., McGuire, S., Ferlez, B., and Kerfeld, C.A. (2019). Structural Characterization of a Synthetic Tandem-Domain Bacterial Microcompartment Shell Protein Capable of Forming Icosahedral Shell Assemblies. ACS Synth Biol 8:668-674.

Sutter, M., Melnicki, M.R., Schulz, F., Woyke, T., and Kerfeld, C.A. (2021). A catalog of the diversity and ubiquity of bacterial microcompartments. Nat Commun 12:3809.

Sutter, M., Roberts, E.W., Gonzalez, R.C., Bates, C., Dawoud, S., Landry, K., Cannon, G.C., Heinhorst, S., and Kerfeld, C.A. (2015). Structural Characterization of a Newly Identified Component of alpha-Carboxysomes: The AAA+ Domain Protein CsoCbbQ. Sci Rep 5:16243.

Takemori, N., Takemori, A., Tanaka, Y., Endo, Y., Hurst, J.L., Gomez-Baena, G., Harman, V.M., and Beynon, R.J. (2017). MEERCAT: Multiplexed Efficient Cell Free Expression of Recombinant QconCATs For Large Scale Absolute Proteome Quantification. Mol Cell Proteomics 16:2169-2183.

Tanaka, S., Kerfeld, C.A., Sawaya, M.R., Cai, F., Heinhorst, S., Cannon, G.C., and Yeates, T.O. (2008). Atomic-level models of the bacterial carboxysome shell. Science 319:1083-1086.

Tsai, Y., Sawaya, M.R., Cannon, G.C., Cai, F., Williams, E.B., Heinhorst, S., Kerfeld, C.A., and Yeates, T.O. (2007). Structural analysis of CsoS1A and the protein shell of the *Halothiobacillus neapolitanus* carboxysome. PLoS Biol 5:e144.

Tsai, Y., Sawaya, M.R., and Yeates, T.O. (2009). Analysis of lattice-translocation disorder in the layered hexagonal structure of carboxysome shell protein CsoS1C. Acta Crystallogr D Biol Crystallogr 65:980-988.

Tsai, Y.C., Lapina, M.C., Bhushan, S., and Mueller-Cajar, O. (2015). Identification and characterization of multiple rubisco activases in chemoautotrophic bacteria. Nat Commun 6:8883.

Tsai, Y.C., Ye, F., Liew, L., Liu, D., Bhushan, S., Gao, Y.G., and Mueller-Cajar, O. (2020). Insights into the mechanism and regulation of the CbbQO-type Rubisco activase, a MoxR AAA+ ATPase. Proc Natl Acad Sci U S A 117:381-387.

Vishniac, W., and Santer, M. (1957). The thiobacilli. Bacteriol Rev 21:195-213.

Whitehead, L., Long, B.M., Price, G.D., and Badger, M.R. (2014). Comparing the *in vivo* function of alpha-carboxysomes and beta-carboxysomes in two model cyanobacteria. Plant Physiol 165:398-411.

Yang, M., Simpson, D.M., Wenner, N., Brownridge, P., Harman, V.M., Hinton, J.C.D., Beynon, R.J., and Liu, L.N. (2020). Decoding the stoichiometric composition and organisation of bacterial metabolosomes. Nat Commun 11:1976.

Yeates, T.O., Kerfeld, C.A., Heinhorst, S., Cannon, G.C., and Shively, J.M. (2008). Protein-based organelles in bacteria: carboxysomes and related microcompartments. Nat Rev Microbiol 6:681-691.

Zhao, Y.Y., Jiang, Y.L., Chen, Y., Zhou, C.Z., and Li, Q. (2019). Crystal structure of pentameric shell protein CsoS4B of Halothiobacillus neapolitanus alpha-carboxysome. Biochem Biophys Res Commun 515:510-515.

bioRxiv preprint doi: https://doi.org/10.1101/2021.12.06.471529; this version posted December 7, 2021. The copyright holder for this preprint (which was not certified by peer review) is the author/funder, who has granted bioRxiv a license to display the preprint in perpetuity. It is made available under aCC-BY 4.0 International license.

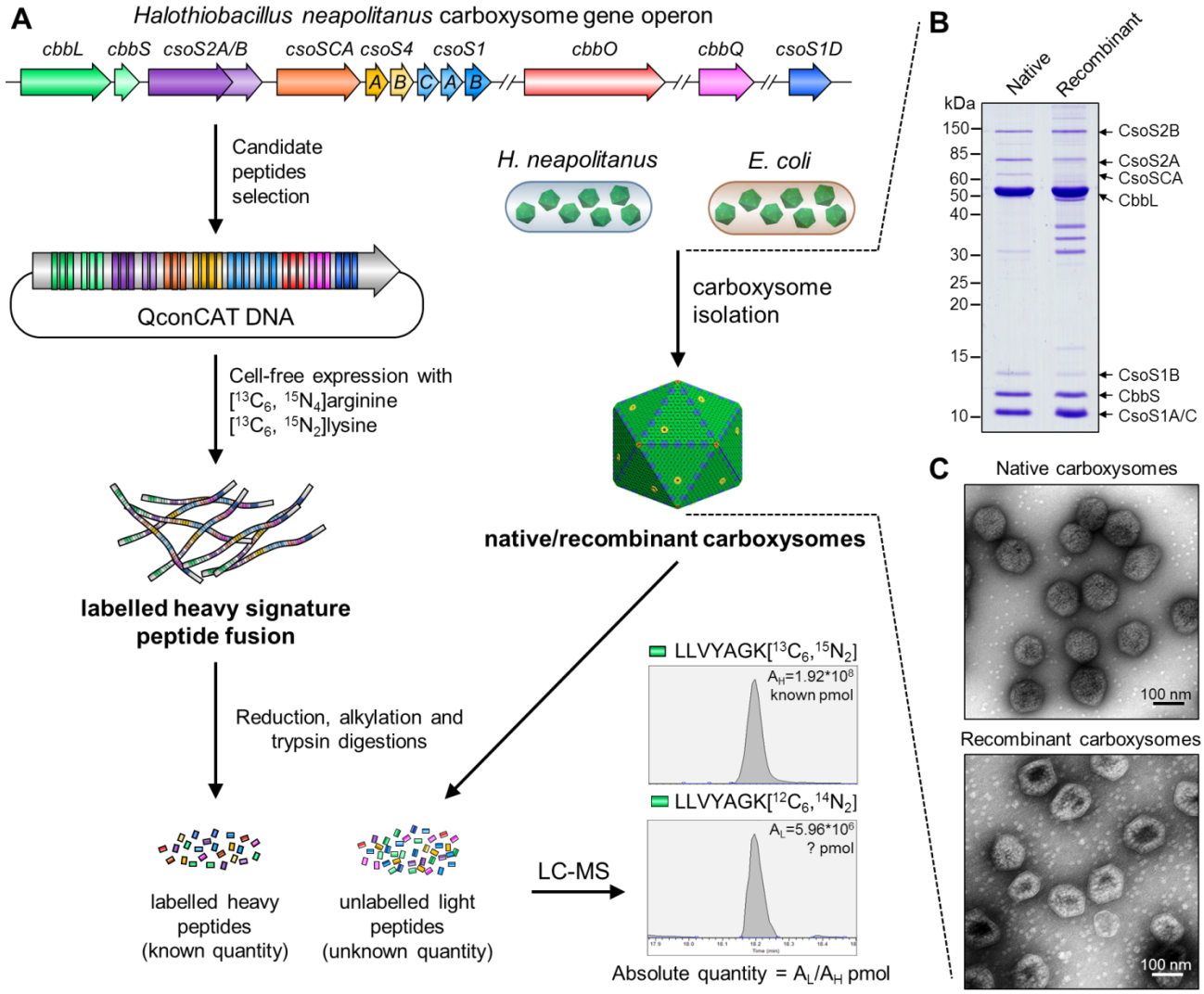

643

644 **Figure 1. Schematic overview of QconCAT strategy.** (**A**) QconCAT DNA fragment was designed
645 from selected gene sequences from the *H. neapolitanus* operon that expresses α-carboxysome proteins.
646 The stable isotopes ([$^{13}C_6$,$^{15}N_4$] arginine and [$^{13}C_6$, $^{15}N_2$] lysine) labelled QconCAT peptide fusion was
647 expressed via a cell-free system, purified and quantified and added to four replicates samples of
648 isolated native/recombinant α-carboxysomes from *H. neapolitanus* and *E. coli*. The absolute quantity
649 and stoichiometry of unlabelled signature peptides for carboxysomal proteins were calculated by LC-
650 MS analysis. One signature peptide for CbbQ, LLVKAGK was shown here as an example. (**B**) SDS-
651 PAGE of isolated native/recombinant α-carboxysomes showing the majority bands of α-carboxysome
652 proteins. (**C**) EM images of isolated native/recombinant α-carboxysomes.

653

bioRxiv preprint doi: https://doi.org/10.1101/2021.12.06.471529; this version posted December 7, 2021. The copyright holder for this preprint (which was not certified by peer review) is the author/funder, who has granted bioRxiv a license to display the preprint in perpetuity. It is made available under aCC-BY 4.0 International license.

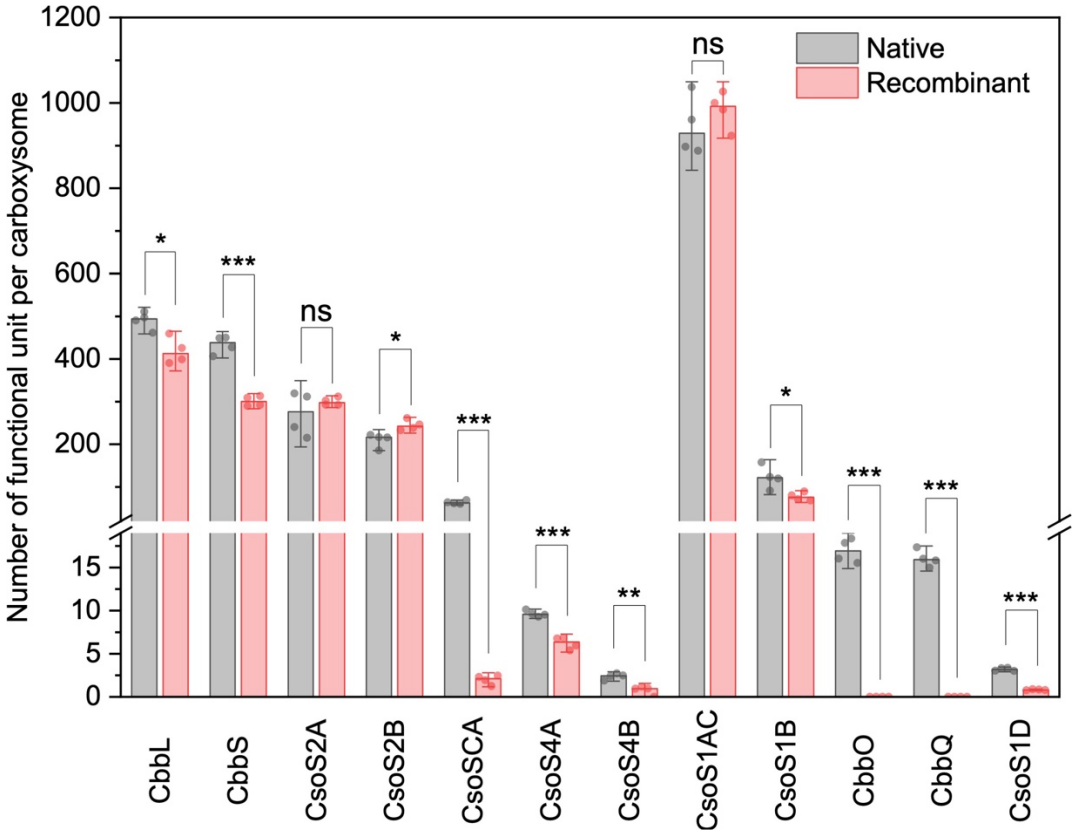

654

655 **Figure 2. Stoichiometry comparison of native and recombinant carboxysomes.** ns, as no statistical
656 significance; *****, $p < 0.05$; ******, $p < 0.01$; *******, $p < 0.001$ using two sample t-test, equal variance not
657 assumed (welch correction). Data are shown as mean ± SD from four biological replicates.

658

bioRxiv preprint doi: https://doi.org/10.1101/2021.12.06.471529; this version posted December 7, 2021. The copyright holder for this preprint (which was not certified by peer review) is the author/funder, who has granted bioRxiv a license to display the preprint in perpetuity. It is made available under aCC-BY 4.0 International license.

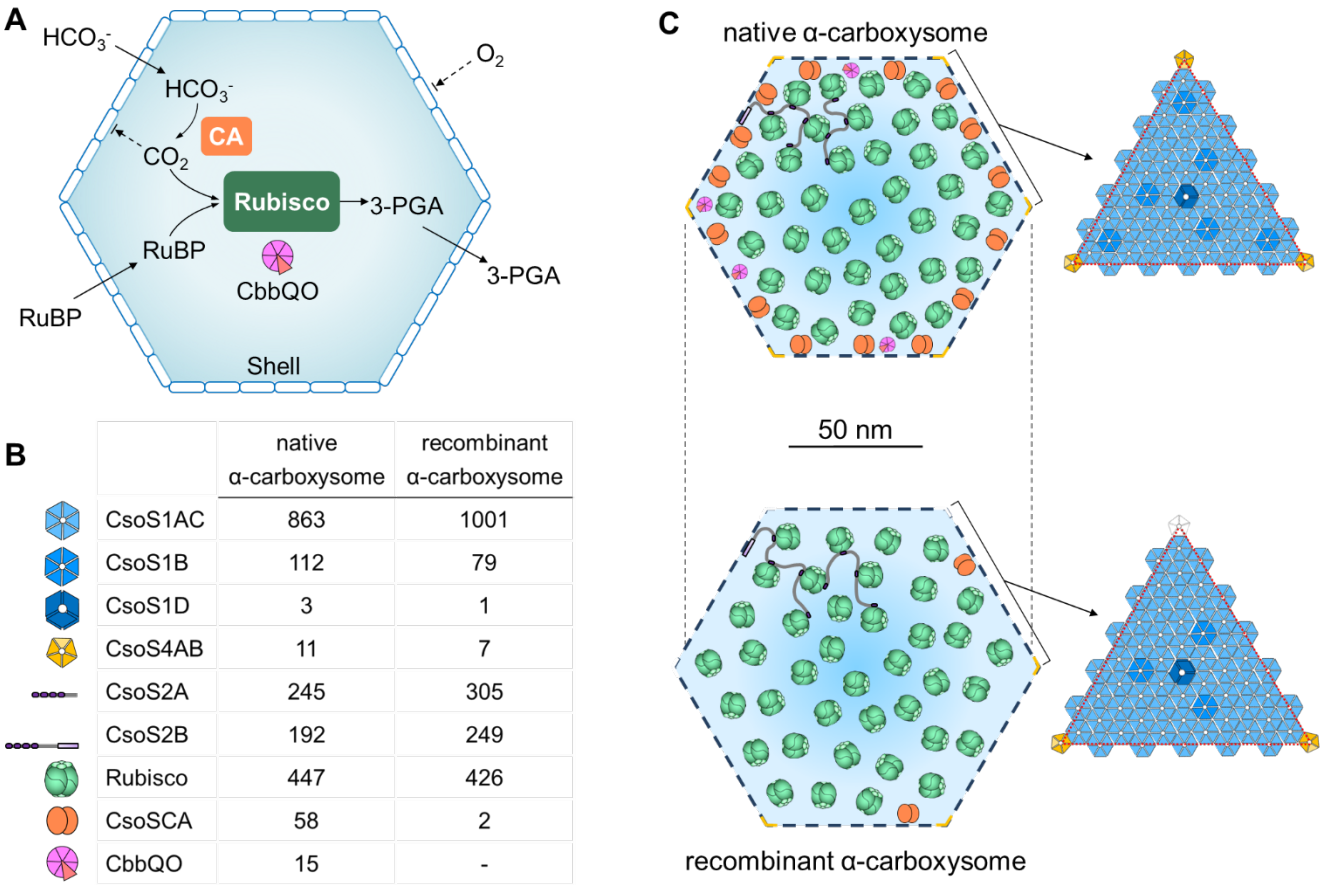

B

	native α-carboxysome	recombinant α-carboxysome
CsoS1AC	863	1001
CsoS1B	112	79
CsoS1D	3	1
CsoS4AB	11	7
CsoS2A	245	305
CsoS2B	192	249
Rubisco	447	426
CsoSCA	58	2
CbbQO	15	-

Figure 3. Structural models of *H. neapolitanus* α-carboxysomes. (**A**) Schematic of the pathways of carbon fixation in the α-carboxysome, including Rubisco activases CbbQO as the structural components; (**B**) The stoichiometry of each structural component within native and recombinant α-carboxysome (see Table 1 and 2). (**C**) Schematic of native and recombinant α-carboxysome structures and shell organizations. The numbers of proteins do not represent actual abundance and is only for illustration purposes.

667 **Table 1. QconCAT quantification of protein components in native α-carboxysomes from *H. neapolitanus*.**

Category	Protein	Structure of functional unit	MW (kDa)	% Total protein by weight	Unit of monomeric protein per carboxysome	Functional unit of multimer per carboxysome
Structural Proteins	CsoS1AC	Hexamer (Tsai et al., 2007; Tsai et al., 2009)	10.0	14.88 ± 1.09	5175.1 ± 378.1	862.5 ± 63
	CsoS1B	Hexamer*	11.3	2.20 ± 0.48	673.3 ± 148.3	112.2 ± 24.7
	CsoS1D	Pseudo-hexamer (Klein et al., 2009)	23.5	0.12 ± 0.01	17.4 ± 1.0	2.9 ± 0.2
	CsoS4A	Pentamer (Tanaka et al., 2008)	8.9	0.11 ± 0.00	43.9 ± 1.6	8.8 ± 0.3
	CsoS4B	Pentamer (Zhao et al., 2019)	8.8	0.03 ± 0.00	10.8 ± 1.6	2.2 ± 0.3
	CsoS2A	Monomer (Cai et al., 2015; Oltrogge et al., 2020)	92.4	6.61 ± 1.26	247.7 ± 47.3	247.7 ± 47.3
	CsoS2B	Monomer (Cai et al., 2015; Oltrogge et al., 2020)	124.2	6.87 ± 0.54	191.5 ± 15.0	191.5 ± 15.0
Catalytic proteins	CbbL	L_8S_8 Hexadecamer (Oltrogge et al., 2020)	52.6	54.36 ± 2.30	3575.7 ± 151.3	447.0 ± 18.9
	CbbS	L_8S_8 Hexadecamer (Oltrogge et al., 2020)	12.9	11.74 ± 0.56	3161.2 ± 150.7	395.1 ± 18.8
	CsoSCA	Dimer (Sawaya et al., 2006)	57.3	1.93 ± 0.12	116.6 ± 7.1	58.3 ± 3.6
	CbbQ	Hexamer (Sutter et al., 2015)	30.1	0.76 ± 0.05	87.8 ± 5.3	14.6 ± 0.9
	CbbO	Monomer (Sutter et al., 2015; Tsai et al., 2020)	88.6	0.39 ± 0.03	15.4 ± 1.3	15.4 ± 1.3
Intact native α-carboxysome			**346.3**			

668 *Based on the structural similarity with CsoS1A/C.

bioRxiv preprint doi: https://doi.org/10.1101/2021.12.06.471529; this version posted December 7, 2021. The copyright holder for this preprint (which was not certified by peer review) is the author/funder, who has granted bioRxiv a license to display the preprint in perpetuity. It is made available under aCC-BY 4.0 International license.

669 **Table 2. QconCAT quantification of protein components in recombinant *H. neapolitanus* α-**
670 **carboxysomes.**

Category	Protein	MW (kDa)	% Total protein by weight	Unit of monomeric protein per carboxysome	Functional Unit of multimer per carboxysome
Structural Proteins	CsoS1AC	10.0	17.80 ± 0.80	6002.9 ± 268.1	1000.5 ± 44.7
	CsoS1B	11.3	1.59 ± 0.19	473.1 ± 56.6	78.8 ± 9.4
	CsoS1D	23.5	0.03 ± 0.00	5.0 ± 0.3	0.8 ± 0.1
	CsoS4A	8.9	0.08 ± 0.01	31.7 ± 3.5	6.3 ± 0.7
	CsoS4B	8.8	0.01 ± 0.01	3.9 ± 2.7	0.8 ± 0.5
	CsoS2A	92.4	8.39 ± 0.26	305.0 ± 9.3	305.0 ± 9.3
	CsoS2B	124.2	9.21 ± 0.47	249.0 ± 12.6	249.0 ± 12.6
Catalytic proteins	CbbL	52.6	53.42 ± 3.96	3408.1 ± 252.4	426.0 ± 31.5
	CbbS	12.9	9.38 ± 0.37	2449.4 ± 96.2	306.2 ± 12
	CsoSCA	57.3	0.07 ± 0.02	4.0 ± 1.1	2.0 ± 0.5
Intact recombinant α-carboxysome		**335.8**			

671

bioRxiv preprint doi: https://doi.org/10.1101/2021.12.06.471529; this version posted December 7, 2021. The copyright holder for this preprint (which was not certified by peer review) is the author/funder, who has granted bioRxiv a license to display the preprint in perpetuity. It is made available under aCC-BY 4.0 International license.

672 **Table 3. Stoichiometric ratios of protein components in α-carboxysomes.** Interior proteins: CbbL,
673 CbbS, CsoS2; Shell proteins: CsoS1, CsoS4.

Ratio of carboxysome proteins	native	recombinant
CbbL:CbbS	8:7.3	8:5.7
CbbL:CsoS2	8:1	8:1.3
CbbL:CsoSCA	30.7:1	846:1
CsoS2A:CsoS2B	1.3:1	1.2:1
CsoS1 hexamer:CsoS2B	5.1:1	4.3:1
CsoS1AC:CsoS1B	7.7:1	12.7:1
CsoS4A:CsoS4B	4.1:1	8.1:1
CbbQ:CbbO	5.7: 1	n/a
shell proteins:internal enzymes	1:1.25	1:1
hexamer:trimmer	336.4:1	1403.5:1
hexamer:pentamer	89.1:1	133.9:1
pentamers per unit of carboxysome	11	7.1

674

bioRxiv preprint doi: https://doi.org/10.1101/2021.12.06.471529; this version posted December 7, 2021. The copyright holder for this preprint (which was not certified by peer review) is the author/funder, who has granted bioRxiv a license to display the preprint in perpetuity. It is made available under aCC-BY 4.0 International license.

Supplemental Information

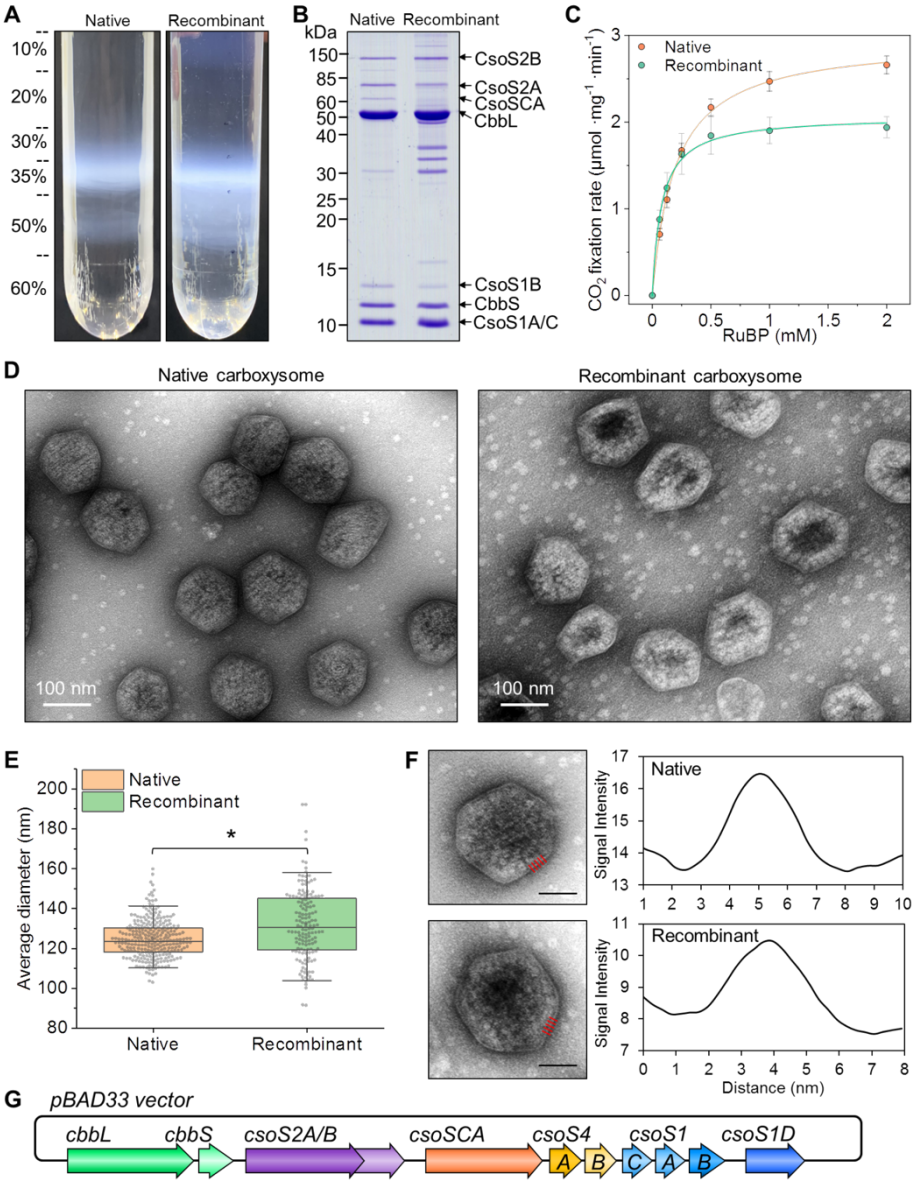

Figure S1. Purification and characterization of native and recombinant α-carboxysomes from *H. neapolitanus* and *E. coli*. **(A)** Sucrose gradient for carboxysome fractions. The milky band between 35%-50% sucrose fraction interface consists of enriched carboxysomes; **(B)** SDS-PAGE of purified carboxysomes isolated from four replicate batches of culture showing the majority bands of α-carboxysome proteins; **(C)** Carbon-fixation kinetics as a function of the RuBP concentrations revealed that native and recombinant carboxysomes possess V_{max} at 2.96 ± 0.09 and 2.07 ± 0.12 μmol·mg^{-1}·min^{-1} and $K_{m(RuBP)}$ at 0.20 ± 0.02 and 0.08 ± 0.02 mM, respectively. Data is shown as mean ± SD from four independent biological replicates; **(D)** TEM image of purified native and recombinant carboxysomes; (**E**) Boxplot distribution for diameters of purified native and recombinant carboxysomes, at 124.6 ± 9.6 nm (n = 272) and 131.8 ± 18.0 nm (n = 152), respectively. Significant difference of average diameter was confirmed with student t-test (p < 0.05); (F) Analysis on the shell thickness of native and recombinant α-carboxysomes. The shell thickness of native and recombinant α-carboxysomes is 5.3 ± 0.6 nm and 5.5 ± 0.8 nm, respectively (n = 100), implicating the single-layer shell architecture. The profile region for measurements were marked by red lines (Scale bar = 50 nm); **(G)** Recombinant α-carboxysome expression cassette containing *cso* operon and *cbbL/S*, plus BMC-T protein encoded gene csoS1D in the pBAD33 vector.

bioRxiv preprint doi: https://doi.org/10.1101/2021.12.06.471529; this version posted December 7, 2021. The copyright holder for this preprint (which was not certified by peer review) is the author/funder, who has granted bioRxiv a license to display the preprint in perpetuity. It is made available under aCC-BY 4.0 International license.

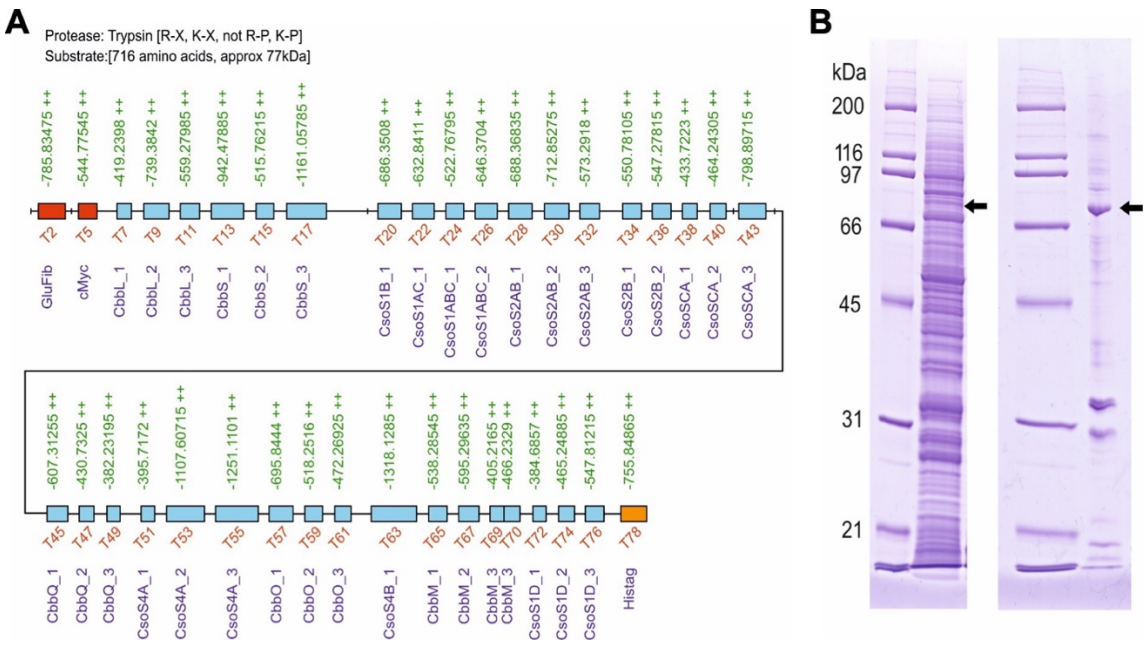

Figure S2. Structure and expression of the *H. neapolitanus* carboxysome QconCAT. (**A**) Schematic representation of the quantification concatamer, for quantification of proteins of interest. 35 peptides in QconCAT are represented by blue boxes. Values for the [M+2H^{2+}] *m/z* peptide ions for the unlabeled QconCAT are aligned above each peptide (green text). The non-target quantification peptides (GluFib and cMyc) and the hexa-histidine tag for QconCAT purification are shaded in red and orange, respectively. (**B**) SDS-PAGE analysis of QconCAT expression and purification. The coding sequence of QconCAT peptide was sub-cloned into the cell-free expression vector pEU-E01-MCS (left). QconCAT was prepared by wheat germ cell-free synthesis in the presence of [$^{13}C_6$,$^{15}N_4$] arginine and [$^{13}C_6$,$^{15}N_2$] lysine and purified by virtue of the hexa-histidine tag (right). The QconCAT is denoted by the arrow.

bioRxiv preprint doi: https://doi.org/10.1101/2021.12.06.471529; this version posted December 7, 2021. The copyright holder for this preprint (which was not certified by peer review) is the author/funder, who has granted bioRxiv a license to display the preprint in perpetuity. It is made available under aCC-BY 4.0 International license.

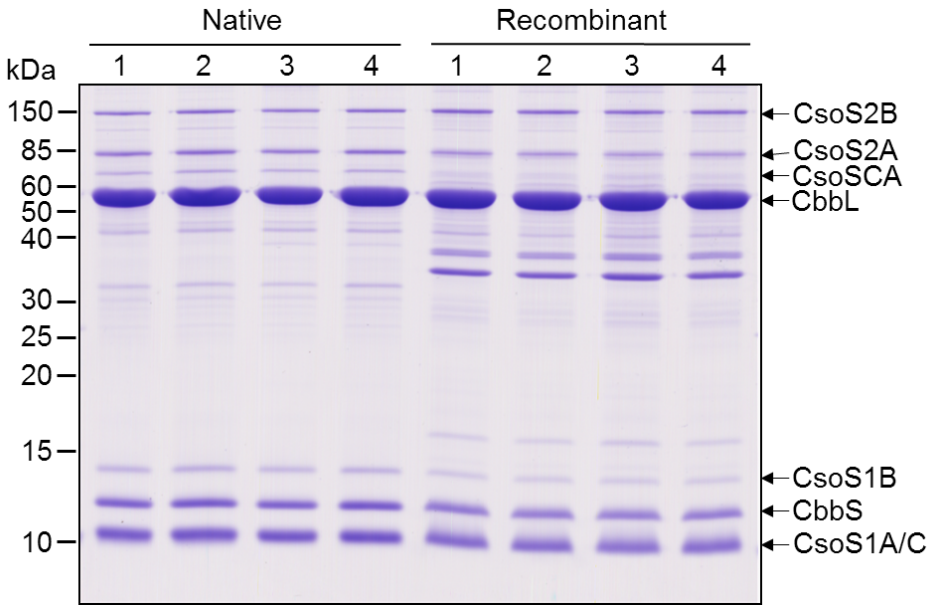

Figure S3. SDS-PAGE of purified carboxysomes from *H. neapolitanus* and *E. coli* with four biological replicates prepared for quantification by QconCAT mass spectrometry. 10 µg proteins are loaded per well.

bioRxiv preprint doi: https://doi.org/10.1101/2021.12.06.471529; this version posted December 7, 2021. The copyright holder for this preprint (which was not certified by peer review) is the author/funder, who has granted bioRxiv a license to display the preprint in perpetuity. It is made available under aCC-BY 4.0 International license.

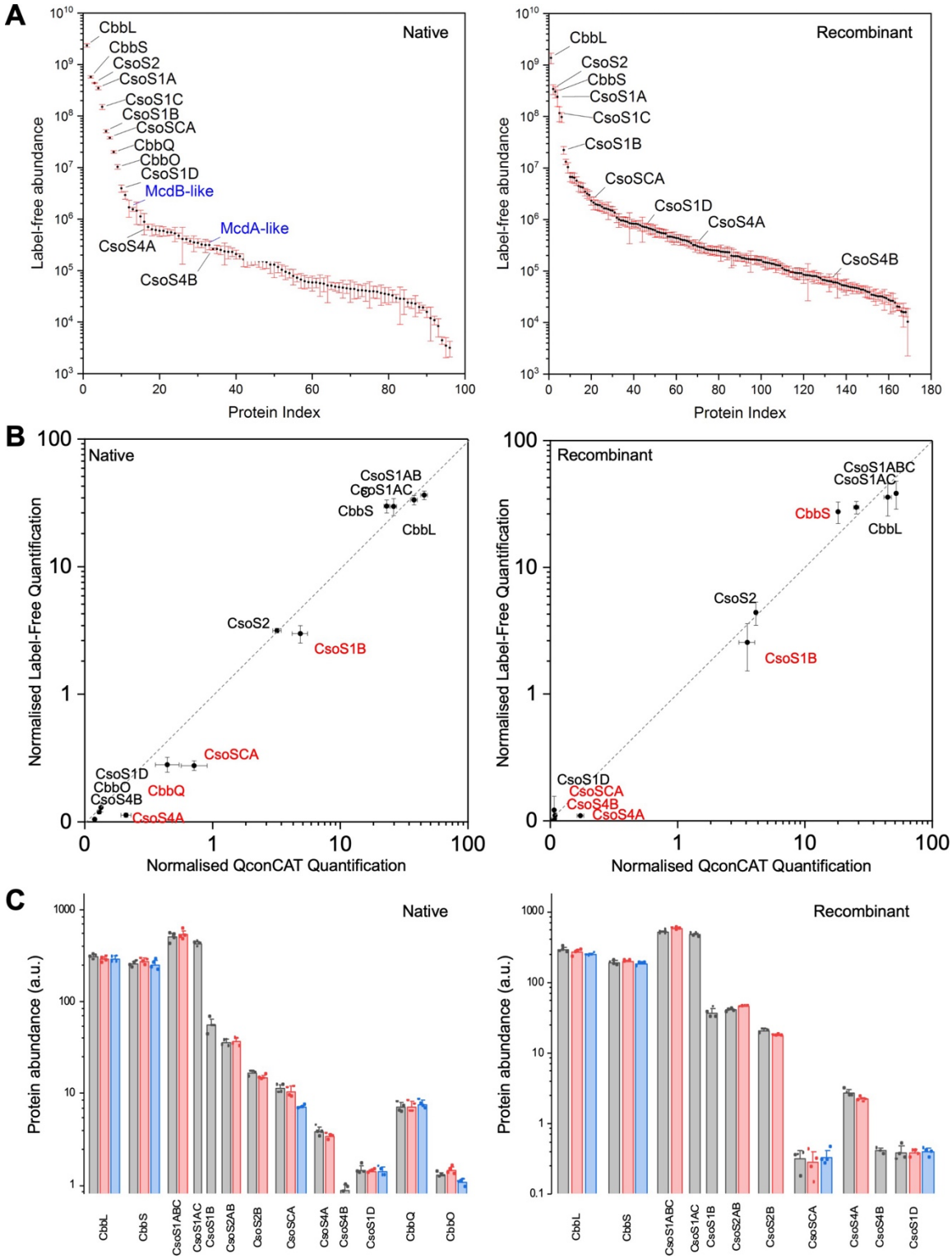

Figure S4. Evaluation of QconCAT and label-free quantification. (**A**) Protein index of all recognized proteins in label-free quantification. In native carboxysome samples, McdAB-like proteins are both detected. The full protein list provided in Supplemental File; (**B**) Comparison of QconCAT and label-free quantification. Quantification was normalized to equal total protein quantity. Proteins with the abundance difference greater than 30% from average are labelled in red; **(C)** Quantification of all QconCAT candidate peptides for *H. neapolitanus* carboxysomes. Overall good agreements are found within candidate peptides for same protein with the exception of peptide 3 of CsoSCA (34 ± 4 % lower than the other two) and CbbO (21 ± 3 %) in native carboxysome samples.

bioRxiv preprint doi: https://doi.org/10.1101/2021.12.06.471529; this version posted December 7, 2021. The copyright holder for this preprint (which was not certified by peer review) is the author/funder, who has granted bioRxiv a license to display the preprint in perpetuity. It is made available under aCC-BY 4.0 International license.

Table S1. Peptides derived from tryptic proteolysis of the QconCAT for carboxysome protein quantification. The flanking sequences that recapitulate the true native primary sequence context, together with additional sequences that are derived from the loop assembly synthesis of the QconCAT are written in gray.

Peptide	M	$[M+H]^+$	$[M+2H]^{++}$	Sequence	Annotation
1	433	434	218	MAGR	N-term
2	1570	1571	786	EGVNDNEEGFFSAR	GluFib
3	356	357	179	LPK	
4	403	404	203	EQK	
5	1088	1089	545	LISEEDLGGR	cMyc
6	1164	1165	583	GSQESSAEDVR	
7	836	837	419	FPLAYVK	CbbL_1
8	718	719	360	TCGILR	
9	1477	1478	739	LSGGDHLHTGTVVGK	CbbL_2
10	658	659	330	LEGANR	
11	1117	1118	559	VALEACVEAR	CbbL_3
12	686	687	344	NQGQIK	
13	1883	1884	942	YAIAQGWSPGIEHVEVK	CbbS_1
14	737	738	370	NSMACR	
15	1030	1031	516	SAYPTHQVK	CbbS_2
16	746	747	374	LVAMWK	
17	2320	2321	1161	LPFFGEQNVDNVLAEIEACR	CbbS_3
18	2398	2399	1200	SAYSAAAAEMADVTGIALGMIETR	
19	599	600	301	GLVVGR	
20	1371	1372	686	SFVGGGYVTVMVR	CsoS1B_1
21	645	646	324	GETIAR	
22	1264	1265	633	VHSEVENILPK	CsoS1AC_1
23	682	683	342	APQLVR	
24	1044	1045	523	GETGAVNAAVR	CsoS1ABC_1
25	662	663	332	AGACER	
26	1291	1292	646	VGDGLVAAHIIAR	CsoS1ABC_2
27	655	656	329	VHSGTR	
28	1375	1376	688	AVPPKPQSQGGPGR	CsoS2AB_1
29	722	723	362	NGYTLR	
30	1424	1425	713	GTSVSGQQLDHAPK	CsoS2AB_2
31	636	637	319	MSGTNK	
32	1145	1146	573	GQSVTGNLVDR	CsoS2AB_3
33	1338	1339	670	SELSAAYAEQNR	
34	1100	1101	551	ITGNDIAPSGR	CsoS2B_1
35	630	631	316	ITGNAR	
36	1093	1094	547	VVETSAFANR	CsoS2B_2
37	658	659	330	NVPDSK	
38	865	866	434	GFLNPYR	CsoSCA_1
39	750	751	376	YVDNLK	
40	926	927	464	GIFGYATAK	CsoSCA_2
41	431	432	217	ALTK	
42	303	304	153	ER	
43	1596	1597	799	FSSLDEQNLLQFR	CsoSCA_3
44	631	632	317	LSVGTR	
45	1213	1214	607	WQDGPLTVAAR	CbbQ_1
46	661	662	332	IGADMR	
47	859	860	431	DALDTVVK	CbbQ_2
48	757	758	380	TFFSTR	
49	762	763	382	LLVYAGK	CbbQ_3
50	1229	1230	615	LIASAAQAEVEK	
51	789	790	396	TLVSTNR	CsoS4A_1

bioRxiv preprint doi: https://doi.org/10.1101/2021.12.06.471529; this version posted December 7, 2021. The copyright holder for this preprint (which was not certified by peer review) is the author/funder, who has granted bioRxiv a license to display the preprint in perpetuity. It is made available under aCC-BY 4.0 International license.

52	688	689	345	IADTNR	
53	2213	2214	1108	IADMGHKPLLVVWEKPGAPR	CsoS4A_2
54	640	641	321	QVAAPR	
55	2500	2501	1251	QVAVDAIGCIPGDWVLCVGSSAAR	CsoS4A_3
56	631	632	317	EAADAR	
57	1390	1391	696	TGENPTLGALFDR	CbbO_1
58	686	687	344	IALQSR	
59	1035	1036	518	TDIPSSPYR	CbbO_2
60	720	721	361	DDNMAR	
61	943	944	472	ELGIALAEK	CbbO_3
62	1190	1191	596	IQQSAASAETGK	
63	2634	2635	1318	VSVACDPIGVPEGCWVFTISGSAAR	
64	703	704	353	FGVPER	
65	1075	1076	538	AIQLFDGPSK	CbbM_1
66	669	670	336	DISHAK	
67	1189	1190	595	IHDIYFPER	CbbM_2
68	644	645	323	AIQSAR	
69	808	809	405	YADLSLK	CbbM_3
70	930	931	466	EEDLIAGGK	
71	751	752	377	HILDVR	
72	767	768	385	AFGNFGR	CsoS1D_1
73	732	733	367	LTMNVR	
74	928	930	465	LGEQVVER	CsoS1D_2
75	621	622	312	AFGAEK	
76	1094	1095	548	AAHVTLIDVR	CsoS1D_3
77	980	981	491	AFGSAAGGSTR	
78	1510	1511	756	DQLALEHHHHHH*	HisTag

47

bioRxiv preprint doi: https://doi.org/10.1101/2021.12.06.471529; this version posted December 7, 2021. The copyright holder for this preprint (which was not certified by peer review) is the author/funder, who has granted bioRxiv a license to display the preprint in perpetuity. It is made available under aCC-BY 4.0 International license.

48 **Table S2. DNA and protein sequences of the recombinant carboxysome QconCAT peptide**

DNA sequences (2151 bp)
ATGGCAGGTCGTGAAGGTGTTAATGATAATGAAGAAGGCTTTTTTAGCGCACGTCTGCCGAAAGAACAGAAACTGATTAGCGAA
GAAGATTTAGGCGGTCGCGGGTCTCAGGAGTCGAGTGCGGAGGATGTTCGTTTTCCGCTGGCATATGTTAAAACCTGTGGTATT
CTGCGTCTTAGTGGTGGTGATCATCTGCATACCGGTACCGTTGTTGGTAAACTGGAAGGTGCCAACCGTGTGGCACTGGAAGC
ATGTGTTGAAGCACGTAATCAGGGTCAGATTAAATATGCGATCGCACAAGGCTGGAGCCCGGGTATTGAACATGTTGAAGTTAA
AAATAGCATGGCATGTCGCAGTGCCTATCCGACCCATCAGGTTAAACTGGTTGCAATGTGGAAACTGCCGTTTTTCGGTGAACA
GAATGTTGATAATGTTCTGGCAGAAATTGAAGCATGTCGTTCAGCCTATTCCGCTGCAGCAGCGGAGATGGCAGATGTTACCGG
TATTGCACTGGGCATGATTGAAACCCGTGGTCTGGTTGTGGGTCGTAGCTTTGTTGGTGGTGGTTATGTTACCGTTATGGTTCG
TGGTGAAACCATTGCCCGTGTGCATAGCGAAGTTGAAAATATTCTGCCGAAAGCACCGCAGTTAGTTCGCGGCGAGACAGGTG
CAGTTAATGCAGCAGTTCGTGCAGGTGCATGTGAACGTGTTGGCGACGGCTTGGTTGCAGCACATATTATTGCACGCGTTCATT
CAGGTACCCGTGCAGTTCCGCCAAAACCACAGAGCCAGGGTGGTCCGGGTCGTAATGGTTATACCCTGCGTGGTACCTCAGTT
TCAGGTCAGCAGCTGGATCATGCACCGAAAATGAGCGGTACCAACAAGGGCCAAAGCGTTACCGGTAATCTGGTTGATCGTAG
CGAACTGTCCGCTGCATACGCGGAGCAGAATCGTATTACCGGCAATGATATTGCACCGAGCGGTCGTATCACAGGTAATGCCA
GAGTTGTTGAAACCAGCGCATTTGCAAATCGTAATGTTCCGGACAGCAAAGGCTTCCTGAATCCGTATCGTTATGTTGATAATCT
GAAAGGTATTTTTGGCTATGCAACCGCAAAAGCACTGACCAAAGAACGTTTTAGCAGCCTGGATGAACAGAACCTTTTACAGTTT
AGACTGAGCGTTGGTACCCGTTGGCAGGATGGTCCGCTGACAGTGGCCGCACGTATTGGTGCAGATATGCGTGATGCACTGGA
TACCGTTGTTAAAACTTTCTTCAGCACACGTTTACTGGTTTATGCAGGTAAACTGATTGCATCCGCTGCACAGGCGGAGGTTGAG
AAAACCCTGGTTAGCACAAATCGTATTGCCGATACCAATCGCATTGCAGATATGGGTCATAAACCGCTGCTGGTTGTTTGGGAA
AAACCGGGTGCACCGCGTCAGGTTGCCGCCCCTCGCCAGGTGGCAGTTGATGCAATTGGTTGTATTCCGGGTGATTGGGTTCT
GTGCGTTGGTAGCAGCGCAGCACGTGAAGCAGCAGATGCACGTACCGGTGAAAATCCGACCCTGGGTGCCCTGTTTGATCGTA
TTGCACTGCAGAGCCGTACAGATATTCCTAGTAGTCCTTATCGTGATGATAATATGGCACGTGAACTGGGTATTGCCCTTGCAGA
GAAAATTCAGCAGTCCGCTGCATCGGCGGAGACAGGTAAAGTTAGCGTTGCATGTGATCCGATTGGCGTTCCTGAAGGTTGCT
GGGTGTTCACCATTAGCGGTAGCGCAGCACGTTTTGGTGTTCCGGAACGTGCCATCCAGTTGTTCGATGGTCCGAGCAAAGAT
ATTAGCCATGCAAAAATTCATGATATTTATTTCCCTGAGCGTGCAATTCAGAGCGCCCGTTATGCAGATCTGAGTCTGAAAGAGG
AAGATCTGATTGCAGGTGGTAAACATATTCTGGATGTTAGAGCATTTGGTAACTTTGGTCGCCTGACCATGAATGTTCGTCTGGG
TGAACAGGTTGTTGAACGTGCATTTGGTGCAGAAAAAGCAGCACATGTTACCCTGATTGATGTTCGCGCCTTTGGTTCCGCTGC
AGGTGGATCTACTAGAGACCAGCTGGCACTGGAACATCATCATCACCATCACTAA

Protein sequence (716 AA)
MAGREGVNDNEEGFFSARLPKEQKLISEEDLGGRGSQESSAEDVRFPLAYVKTCGILRLSGGDHLHTGTVVGKLEGANRVALEACVE
ARNQGQIKYAIAQGWSPGIEHVEVKNSMACRSAYPTHQVKLVAMWKLPFFGEQNVDNVLAEIEACRSAYSAAAAEMADVTGIALGMI
ETRGLVVGRSFVGGGYVTVMVRGETIARVHSEVENILPKAPQLVRGETGAVNAAVRAGACERVGDGLVAAHIIARVHSGTRAVPPKP
QSQGGPGRNGYTLRGTSVSGQQLDHAPKMSGTNKGQSVTGNLVDRSELSAAYAEQNRITGNDIAPSGRITGNARVVETSAFANRNV
PDSKGFLNPYRYVDNLKGIFGYATAKALTKERFSSLDEQNLLQFRLSVGTRWQDGPLTVAARIGADMRDALDTVVKTFFSTRLLVYAG
KLIASAAQAEVEKTLVSTNRIADTNRIADMGHKPLLVVWEKPGAPRQVAAPRQVAVDAIGCIPGDWVLCVGSSAAREAADARTGENPT
LGALFDRIALQSRTDIPSSPYRDDNMARELGIALAEKIQQSAASAETGKVSVACDPIGVPEGCWVFTISGSAARFGVPERAIQLFDGPS
KDISHAKIHDIYFPERAIQSARYADLSLKEEDLIAGGKHILDVRAFGNFGRLTMNVRLGEQVVERAFGAEKAAHVTLIDVRAFGSAAGGS
TRDQLALEHHHHHH

49

bioRxiv preprint doi: https://doi.org/10.1101/2021.12.06.471529; this version posted December 7, 2021. The copyright holder for this preprint (which was not certified by peer review) is the author/funder, who has granted bioRxiv a license to display the preprint in perpetuity. It is made available under aCC-BY 4.0 International license.

Table S3. Calculation of carboxysome surface area, shell hexamer content, and carboxysome diameter.

	native α-carboxysome (*n* = 272)	recombinant α-carboxysome (*n* = 152)
EM-measured diameter (nm)	124.6 ± 9.6	131.8 ± 18.0
Radius of circumscribed sphere (nm)	62.3 ± 4.8	65.9 ± 9.0
Facet side length (nm)	65.5 ± 5.0	69.3 ± 9.4
Carboxysome surface area (nm^2)	37407.3 ± 5864.6	42354.8 ± 11745.1
CsoS1 hexamer width (nm)*	6.64	6.64
CsoS1 hexamer area (nm^2)*	38.9	38.9
CsoS4 pentamer area (nm^2)*	30.3	30.3
All facet hexamer counts	977.6 ± 150.9	1080.2 ± 302.1
Estimated Rubisco counts per carboxysome[&]	410.7 ± 101.8	491.4 ± 216.1

*CsoS1 and CsoS4 width/area obtained from previous publications (Tanaka et al., 2008; Tsai et al., 2007);

[&]Assumed packing densities of 74% (Kepler packing) (Whitehead et al., 2014) in the proposed carboxysome model based on the measured carboxysome diameters.

bioRxiv preprint doi: https://doi.org/10.1101/2021.12.06.471529; this version posted December 7, 2021. The copyright holder for this preprint (which was not certified by peer review) is the author/funder, who has granted bioRxiv a license to display the preprint in perpetuity. It is made available under aCC-BY 4.0 International license.

Table S4. Absolute protein abundance per native and recombinant carboxysome based on 12-pentamer occupation and surface area coverage.

Protein	native α-carboxysome		recombinant α-carboxysome	
	12 pentamers	CsoS1 coverage*	12 pentamers	CsoS1 coverage*
CbbL	490.2 ± 20.7	447.0 ± 18.9	717.0 ± 53.1	426.0 ± 31.5
CbbS	433.4 ± 20.7	395.1 ± 18.8	515.3 ± 20.2	306.2 ± 12
CsoS1AC	945.9 ± 69.1	**862.5 ± 63**	1683.9 ± 75.2	**1000.5 ± 44.7**
CsoS1B	123.1 ± 27.1	**112.2 ± 24.7**	132.7 ± 15.9	**78.8 ± 9.4**
CsoS2A	271.7 ± 51.8	247.7 ± 47.3	513.3 ± 15.7	305 ± 9.3
CsoS2B	210 ± 16.4	191.5 ± 15	419.1 ± 21.3	249 ± 12.6
CsoSCA	63.9 ± 3.9	58.3 ± 3.6	3.4 ± 0.9	2.0 ± 0.5
CsoS4A	**9.6 ± 0.4**	8.8 ± 0.3	**10.7 ± 1.2**	6.3 ± 0.7
CsoS4B	**2.4 ± 0.4**	2.2 ± 0.3	**1.3 ± 0.9**	0.8 ± 0.5
CsoS1D	3.2 ± 0.2	**2.9 ± 0.2**	1.4 ± 0.1	**0.8 ± 0.1**
CbbQ	16 ± 1	14.6 ± 0.9	N/A	N/A
CbbO	16.9 ± 1.4	15.4 ± 1.3	N/A	N/A

*Based on surface area of ideal icosahedral with diameters measured from EM, 124.6 ± 9.6 nm (*n* = 272) and 131.8 ± 18.0 nm (*n* = 152) for native and recombinant carboxysomes, respectively. Value used for standardization was displayed in bold. Calculation was described in Methods.

bioRxiv preprint doi: https://doi.org/10.1101/2021.12.06.471529; this version posted December 7, 2021. The copyright holder for this preprint (which was not certified by peer review) is the author/funder, who has granted bioRxiv a license to display the preprint in perpetuity. It is made available under aCC-BY 4.0 International license.

Table S5. Primer sets used for pBAD33-CBS1D construction

Primer name	Sequence (5'-3')
S1D-R	GCTACGCCTGAATAAGTGCTGCAGGCGGCCCTGTTCGACTTAAGCATTATGGC GGCCGCTTAGAACCCTTCAGCGCGACGCG
S1D-F	GTTTAACTTTAAGAAGGAGATATACAATGGCAGTTAAAAAGTATAGTGCTGGTG
pBAD33-R	TGTATATCTCCTTCTTAAAGTTAAACAAAATTATTTCTAGAGG
pBAD33-F	GCACTTATTCAGGCGTAGCAAC

Supplemental References

Tanaka, S., Kerfeld, C.A., Sawaya, M.R., Cai, F., Heinhorst, S., Cannon, G.C., and Yeates, T.O. (2008). Atomic-level models of the bacterial carboxysome shell. Science 319:1083-1086.

Tsai, Y., Sawaya, M.R., Cannon, G.C., Cai, F., Williams, E.B., Heinhorst, S., Kerfeld, C.A., and Yeates, T.O. (2007). Structural analysis of CsoS1A and the protein shell of the *Halothiobacillus neapolitanus* carboxysome. PLoS Biol 5:e144.

Whitehead, L., Long, B.M., Price, G.D., and Badger, M.R. (2014). Comparing the *in vivo* function of alpha-carboxysomes and beta-carboxysomes in two model cyanobacteria. Plant Physiol 165:398-411.